Oxidations of organic and inorganic substrates by superoxo-, hydroperoxo-, and oxo-compounds of the transition metals.

by

Michael John Vasbinder

A dissertation submitted to the graduate faculty

in partial fulfillment of the requirements for the degree of

DOCTOR OF PHILOSOPHY

Major: Inorganic Chemistry

Program of Study Committee:
Andreja Bakac, Co-major Professor
James H. Espenson, Co-major Professor
Robert J. Angelici
William S. Jenks
Jacob S. Petrich

Iowa State University

Ames, Iowa

2006

TABLE OF CONTENTS

IS-T 2327

GENERAL INTRODUCTION

Introduction

The unifying theme in the three following research chapters is oxygen. The goal of this research is to understand the reactivity of complexes with oxygen coordinated to transition metal centers. This is accomplished through careful studies of the thermodynamics and kinetics of reactions involving metal-oxygen species, with special emphasis placed on the mechanism of these reactions. It is hoped that such studies of small, well-defined, and relatively long-lived complexes will provide insight into their reactivity in far more complicated environments, such as in vivo or in catalytic processes. Both compounds derived from molecular oxygen coordination to transition metal centers (Chapters I and II) as well as a high oxidation state metal-oxo species, and subsequent catalytic redox chemistry, have been studied (Chapter III). The activation of oxygen is of tremendous importance because of the roles it plays in Nature and the roles it may play, and to an extent already does play, in economics. It is also an interesting topic for many scientists and the agencies that fund them for these same reasons.

Oxygen activation most often occurs during its coordination to a transition metal center, as depicted below.

$$M^{II n+} + O_2 \longrightarrow M^{III}OO^{n+}$$

$$M^{III}OO^{n+} \xrightarrow{e^- \; H^+} M^{III}OOH^{n+} \xrightarrow[-H_2O]{e^- \; H^+} M^{IV}O^{n+}$$

superoxometal — hydroperoxometal — metal-oxo

This stepwise reduction of oxygen at a metal center generates many reactive intermediates and provides the driving force for many oxygen catalyzed reactions. These reactive intermediates include superoxometal species, hydroperoxo- and alkylperoxometal species, and high-valent metal-oxo compounds.

In Nature, the mono- (eq 1) and dioxygenase (eq 2) enzymes catalyze an enormous number of biological oxidations using activated molecular oxygen as the oxidant.

$$R\text{-}H + 2e^- + O_2 + 2H^+ \rightarrow R\text{-}OH + H_2O \quad (1)$$

$$2S + O_2 \rightarrow 2SO \quad \text{where S is a substrate} \quad (2)$$

The monoxygenase cyctochrome-P450 is one of the most important and best understood examples of such enzymes,[1] being able to carry out difficult hydroxylations of hydrocarbons under physiological conditions. P450 is also involved in the metabolism of most pharmaceuticals.[2] Through extensive study, the oxygen-rebound mechanism has been developed to explain P450 reactivity.[3]

$$R\text{-}H + Por^{\bullet+}Fe^{IV}O^{\bullet} \rightarrow \{Por^{\bullet+}Fe^{III}\text{-}OH + R^{\bullet}\} \rightarrow PorFe^{III} + R\text{-}OH \quad (3)$$

Free-radical rearrangements consistent with this mechanism are observed.[4] Model studies of heme and non-heme oxidases are also very common, and involve all the metal oxygen intermediates mentioned above.[5-8] The heme models are typically designed to study P450, and P450's reactions have been successfully mimicked by porphyrin complexes of Fe^{III}, Cr^{III}, Mn^{III}, and Ru^{III}.[9-11], as well as Fe^{II} and H_2O_2,[12] and even the entire system with iron porphyrin as catalyst, O_2 as oxidant, and Zn powder reductant.[13,14] The non-heme studies are generally aimed at emulating the structure and mimicking the reactivity of the enzymes methane monooxygenase (MMO) and ribonucleotide reductase (RNR).[15]

Commercially, oxygen is the most attractive alternative when compared to costly and environmentally unfriendly oxidants such as permanganate and chromate. Other cheap and relatively benign oxidants, such as ozone, hydrogen peroxide, and alkyl peroxides such as *tert*-butylhydroperoxide, are themselves produced from oxygen. Metal-catalyzed autoxidation is already used in the MC process for the production of terephthalic acid from *p*-xylene, the largest commercial oxidation process.[16] The worldwide demand for terephthalic acid in 2006 exceeded 2.7×10^7 tonnes,[17] most of which is destined to be the monomer in polyethylene terephthalate polyester, common in bottles. A mixture of Co^{II}, Mn^{II}, (usually as diacetate salts) and Br^- (from NaBr or HBr) serves as the catalyst for the overall reaction, as shown in eq 4 below.

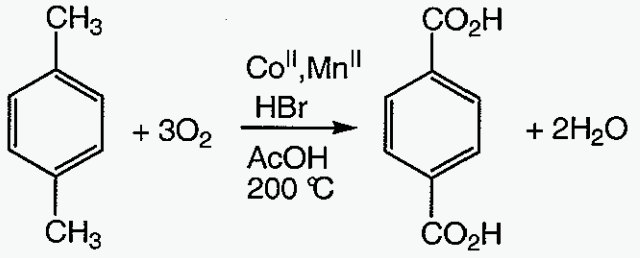

(4)

The mechanism of this complex reaction is equally complex, but is understood to involve initiation by Co^{III} produced *in situ* (eq 5), and sustained by the reaction of alkylperoxo radicals with Co^{II}, Mn^{II}, and Br^-.[18,19]

$$ArCH_2\text{-}H + Co^{III} + O_2 \rightarrow Co^{II} + ArCH_2OO\bullet + H^+ \quad (5)$$

$$ArCH_2OO\bullet + M^{II} + H^+ \rightarrow M^{III} + ArCH_2OOH \rightarrow \text{Products} \quad (6)$$

$$ArCH_2OO\bullet + Br^- + H^+ \rightarrow Br\bullet + ArCH_2OOH \rightarrow \text{Products} \qquad (7)$$

Metal-oxo species are also important oxidants in commercially significant heterogeneous autoxidations. In the oxidation of propylene to acrolein, a molybdenum oxide surface catalyzes the reaction by serving as the active oxidant. Vanadium oxide plays the same role in the conversion of butane to maleic anhydride (eq 8).[20]

$$C_4H_{10} + 3.5O_2 \xrightarrow[\sim 400\ ^\circ C]{(VO)_2P_2O_7} \text{maleic anhydride} + 4H_2O \qquad (8)$$

Metal-oxo species also play an important role as catalysts in oxygen-atom transfer processes (OAT). Oxygen-atom transfers are two-electron redox reactions, accomplished by the formal movement of an oxygen atom from an oxidant XO to a reductant, R.[21]

$$XO + R \rightarrow X + RO \qquad (9)$$

These reactions are also important in Nature and in industry. A biological example can be found in the molybdenum-containing oxotransferase enzymes, such as sulfite oxidase or dimethylsulfoxide reductase, both of which add or remove an oxygen atom from their respective substrate.[22] These enzymes feature pterin dithiolate $Mo^{IV/VI}$ -oxo at their active sites. Model studies[23] have successfully mimicked he structure and reactivity of these enzymes.[24]

An industrial example of OAT is found in the Halcon Oxirane process, where propylene is selectively oxidized to its epoxide, propylene oxide, by *tert*-butylhydroperoxide and a metal catalyst. The market for propylene oxide in 2003

was over 5 x 10^6 tonnes per year.[25] The metal catalyst is thought to be a d^0 metal-oxo species with bound *tert*-butylhydroperoxide (TBOOH) that transfers the oxygen to propylene in an analogous step to the enzymatic reaction above.[20]

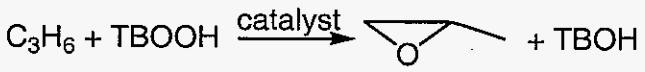

(10)

The mechanism involves either or both an electrophilic attack of the olefin directly on the metal-oxo/hydroperoxo intermediate,[26] or a stepwise process that involves coordination to the metal center followed by formation metallacyclic organometallic intermediate.[27]

Dissertation Organization

This thesis is organized into three self-contained chapters, each with its own figures, tables, and references. Manuscripts have been submitted for Chapters I and II. Chapter III has been published in *Organometallics*. All the work presented in this thesis was performed by the author.

References

(1) Woggon, W.-D. *Top. Curr. Chem.* **1997**, *184*, 39-96.

(2) Guengerich, F. P. *Biol. Chem.* **2002**, *383*, 1553-1564.

(3) Groves, J. T. *J. Chem. Educ.* **1985**, *62*, 928-931.

(4) Auclair, K.; Hu, Z.; Little, D. M.; Ortiz de Montellano, P. R.; Groves, J. T. *J. Am. Chem. Soc.* **2002**, *124*, 6020-6027.

(5) Shan, X.; Que, L., Jr. *Proc. Natl. Acad. Sci. U.S.A* **2005**, *102*, 5340-5345.

(6) Lee, D.; Pierce, B.; Krebs, C.; Hendrich, M. P.; Huynh, B. H.; Lippard, S. J. *J. Am. Chem. Soc.* **2002**, *124*, 3993-4007.

(7) Rivera, M.; Caignan, G. A.; Astashkin, A. V.; Raitsimring, A. M.; Shokhireva, T. K.; Walker, F. A. *J. Am. Chem. Soc.* **2002**, *124*, 6077-6089.

(8) De Angelis, F.; Jin, N.; Car, R.; Groves, J. T. *Inorg. Chem.* **2006**, *45*, 4268-4276.

(9) Groves, J. T.; Bonchio, M.; Carofiglio, T.; Shalyaev, K. *J. Am. Chem. Soc.* **1996**, *118*, 8961-8962.

(10) Groves, J. T.; Watanabe, Y. *J. Am. Chem. Soc.* **1988**, *110*, 8443-8452.

(11) Groves, J. T.; Adhyam, D. V. *J. Am. Chem. Soc.* **1984**, *106*, 2177-2181.

(12) Belova, V. S.; Khenkin, A. M.; Shilov, A. E. *Kinet. Katal.* **1988**, *29*, 1279.

(13) Karasevich, E. I.; Khenkin, A. M.; Shilov, A. E. *J. Chem. Soc., Chem. Comm.* **1987**, 731-732.

(14) Karasevich, E. I.; Khenkin, A. M.; Shilov, A. E. *Dokl. Akad. Nauk SSSR* **1987**, *295*, 639-642.

(15) Tshuva, E. Y.; Lippard, S. J. *Chem. Rev.* **2004**, *104*, 987-1011.

(16) Parshall, G. W.; Ittel, S. D. *Homogeneous Catalysis*; 2nd ed.; Wiley-Interscience: New York, 1992.

(17) http://www.bp.com/sectiongenericarticle.do?categoryId=9003710&contentId=7006848. Accessed on 6/29/06, BP p.l.c., 2006.

(18) Partenheimer, W. *Catal. Today* **1995**, *23*, 69-157.

(19) Cincotti, A.; Orru, R.; Cao, G. *Catal. Today* **1999**, *52*, 331-347.

(20) Ebner, J.; Riley, D. In *Active Oxygen in Chemistry*; Foote, C. S., Valentine, J. S., Greenberg, A., Liebman, J. F., Eds.; Chapman & Hall: London, 1995, 204-249.

(21) Holm, R. H. *Chem. Rev.* **1987**, *87*, 1401-1449.

(22) Young, C. G.; Wedd, A. G. *Chem. Comm.* **1997**, 1251-1257.

(23) Enemark, J. H.; Cooney, J. J. A.; Wang, J.-J.; Holm, R. H. *Chem. Rev.* **2004**, *104*, 1175-1200.

(24) Lim, B. S.; Willer, M. W.; Miao, M.; Holm, R. H. *J. Am. Chem. Soc.* **2001**, *123*, 8343-8349.

(25) http://www.lyondell.com/html/products/products/po.shtml. Accessed on 6/29/06, Lyondell Chemical Company, 2006

(26) Sharpless, K. B.; Teranishi, A. Y.; Backvall, J. E. *J. Am. Chem. Soc.* **1977**, *99*, 3120-3128.

(27) Mimoun, H.; Mignard, M.; Brechot, P.; Saussine, L. *J. Am. Chem. Soc.* **1986**, *108*, 3711-3718.

CHAPTER I. THE REACTION OF HYDROPEROXOMETAL COMPLEXES WITH SUPEROXO- AND HIGH-VALENT METAL OXO COMPLEXES OF CHROMIUM.

Michael J. Vasbinder and Andreja Bakac.

A manuscript submitted to the *Journal of the American Chemical Society.*

Abstract

The superoxochromium ions $LCr(H_2O)OO^{2+}$ (L = $(H_2O)_4$ and [14]aneN_4) and chromyl ion $Cr^{IV}_{aq}O^{2+}$ were shown to oxidize hydroperoxometal ions of Rh and Co to their corresponding superoxides. Kinetic isotope effects support hydrogen atom transfer from hydroperoxo- to superoxometal as the rate limiting step. Rate constants were determined and lie in the range of 17 to 130 M^{-1} s^{-1} for $LCr(H_2O)OO^{2+}$ as oxidant and 10^3-10^4 M^{-1} s^{-1} for $Cr^{IV}_{aq}O^{2+}$ as oxidant. These rate constants are compared against other known hydrogen atom transfer reactions of hydroperoxo-, superoxo-, and oxo-metal ions.

Introduction

The following reactions have been studied:

$$LMOO^{2+} + LM'OOH^{2+} \rightarrow LMOOH^{2+} + LM'OO^{2+} \quad (1)$$

$$LM^{IV}O^{2+} + LM'OOH^{2+} + H^{+} \rightarrow LM^{3+} + LM'OO^{2+} \quad (2)$$

where M is a transition metal complex of either Cr, Rh or Co with a superoxo, hydroperoxo, or oxo-ligand. The reaction of the superoxo and hydroperoxyl radical with hydrogen peroxide in solution has been studied in depth.[1] It is clear that this reaction does not yield products analogous to those in eq 1.

$$H_2O_2 + HO_2 \rightarrow \bullet OH + H_2O + O_2 \quad (3)$$

To our knowledge, no examples of a superoxometal complex reacting with a hydroperoxometal complex are known. In addition to our basic interest in understanding redox reactions of superoxo- and hydroperoxometal complexes, these species are important in both biological and industrial contexts.

Superoxo and peroxo complexes of the transition metals are important intermediates in autoxidations catalyzed by transition metals. An example is found in $LCo^{III}OOR$ and similar intermediates in the DuPont K/A oil process for cyclohexane autoxidation to cyclohexanone and cyclohexanol. This reaction is carried out on a large scale, eventually producing the adipic acid monomer used in the production of nylon 6,6.[2,3] The metal controls the decomposition of the key organic intermediate, $C_6H_{11}OOH$, into alkoxyl and peroxyl radicals that sustain the reaction, as shown in Scheme 1.

Scheme 1.

$$Co^{3+} + C_6H_{11}OOH \longrightarrow Co^{2+} + C_6H_{11}OO\bullet + H^+$$

$$Co^{2+} + C_6H_{11}OOH \longrightarrow Co^{3+} + C_6H_{11}O\bullet + OH^-$$

$$C_6H_{11}OOH \longrightarrow C_6H_{10}O + H_2O$$

$$2C_6H_{11}OO\bullet \longrightarrow C_6H_{10}O + C_6H_{11}OH + O_2$$

Oxygen coordination and subsequent stepwise reduction at a metal are key steps in biological systems that use oxygen. The active site of biological oxygen carriers hemoglobin and myoglobin are superoxoiron complexes. Both superoxo- and peroxometal ions can be seen in the active site of both heme and non-heme[4] iron-containing oxidase enzymes, as well as being responsible for the antibiotic and antitumor activity of bleomycin. In the heme oxidases, both superoxo- and peroxometal ions are important transients in enzymatic activity, either acting as the oxidant for substrates themselves, or being further oxidized to even more powerful terminal oxidants, usually a metal-oxo species in a high oxidation state. A hydroperoxoiron is the "active" species in bleomycin. It and its high-valent metal oxo derivatives cleave DNAs sugar backbone in both cancer cells and bacteria.[5,6]

We expect superoxometal and high-valent metal-oxo complexes, such as the aquasuperoxochromium ion ($Cr_{aq}OO^{2+}$/ $Cr_{aq}OOH^{2+}$ E^o = 1.03 V vs. NHE)[7] and chromyl ion, $Cr^{IV}{}_{aq}O^{2+}$, to oxidize hydroperoxometal complexes, likely into their corresponding superoxide, as in eq 1 and 2. Possible mechanisms for the conversion of a superoxometal complex to the corresponding hydroperoxometal complex are hydrogen atom transfer, proton coupled electron transfer, and electron transfer followed by subsequent protonation. Representations of the various complexes studied are shown in Chart 1.

Chart 1.

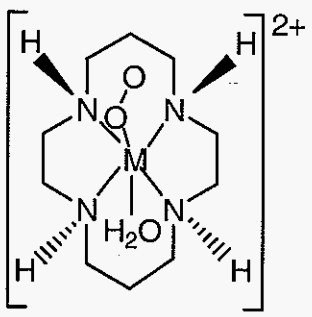

$L^1M^{III}(H_2O)OO^{2+}$

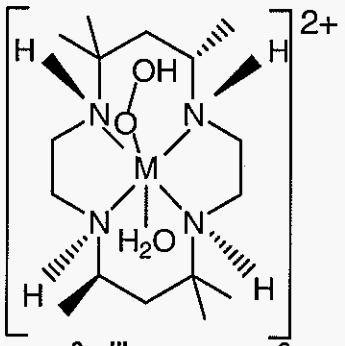

$L^2M^{III}(H_2O)OOH^{2+}$

M = Cr, Co, Rh

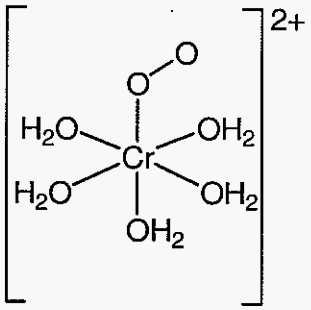

$Cr^{III}{}_{aq}OO^{2+}$

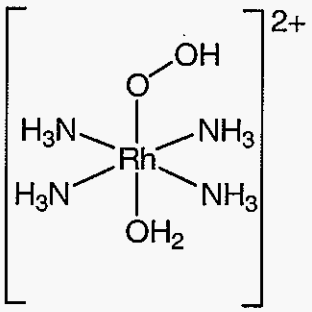

$Rh^{III}(NH_3)_4(H_2O)OOH^{2+}$

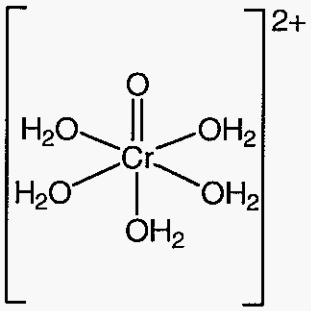

$Cr^{IV}{}_{aq}O^{2+}$

Experimental

Metal complexes were prepared by literature procedures, as follows:

Preparation of *trans*-$[L^1Cr(H_2O)_2](CF_3SO_3)_3$ L^1= [14]aneN$_4$

An argon-saturated suspension of 1 g of *trans*-[$L^1Cr(Cl)_2]Cl$ in 50 mL of 0.1 M CF_3SO_3H was placed on Zn/Hg under argon. The gray suspension turned into a pink solution of *trans* – $L^1Cr(Cl)(H_2O)^{2+}$ (and over another 15 min. to cherry-red *trans* – $L^1Cr\ (H_2O)_2^{2+}$ This was transferred into a beaker and bubbled with a stream of O_2 for a few minutes to generate *trans* – $L^1Cr(H_2O)_2^{3+}$, which was then purified by ion exchange chromatography on SP-Sephadex C-25. The dichloro and monochloro complexes were eluted with 0.1M CF_3SO_3H, and the major peach band of *trans* – $L^1Cr(H_2O)_2^{3+}$ was eluted with 1 M CF_3SO_3H, leaving a dark band on the column. Multiple fractions were taken and standardized spectrophotometrically ($\varepsilon_{508\ nm}$ = 17.2 $M^{-1}\ cm^{-1}$).[8]

Preparation of *trans*-[$L^1Rh(H_2O)_2H](CF_3SO_3)_2$

A 0.53 g sample of *trans*-[$L^1Rh(Cl)_2]Cl$ was dissolved in 15 mL of deionized H_2O. The yellow solution was saturated with argon and warmed to ~60 ℃, and ~200 mg of Zn powder was slowly added over several minutes, causing visible hydrogen evolution. The reaction mixture was stirred for an additional 45 min. until most of the color had faded. The excess zinc was removed by filtration, and the faint yellow solution was concentrated by rotovap. The white solid product, *trans*-{[$L^1Rh(Cl)H]]_2(ZnCl_4)$, was filtered and washed with acetone. This was later dissolved in dilute $HClO_4$ and recrystalized from a large excess of $LiCF_3SO_3$, yielding the desired product.[9]

Preparation of *trans*-$[L^2Co(H_2O)_2](CF_3SO_3)_2$ L^2 = *meso*-Me$_6$-[14]aneN$_4$

A 0.91 g sample of $CoCl_2 \bullet 6\ H_2O$ was dissolved in 5 mL of 2,2-dimethoxypropane and 2 mL DMF. This was purged with argon and stirred for ~ 1 hr, during which the

pink suspension became a dark blue solution. This solution was added to 0.53 g L^2 in 9 mL argon-saturated DMF which was then heated to ~80 °C and maintained at this temperature for ~1 hr, during which time a light blue solid precipitated. The blue solid product was filtered under a stream of argon and washed with MeOH : $2Et_2O$ and dried with a stream of Ar. 0.41 g [$L^2Co(Cl)_2]Cl$ was recovered, 40% yield. This was later recrystalized from a large excess of $LiCF_3SO_3$, yielding $[L^2Co(H_2O)_2](CF_3SO_3)$.[10]

Superoxochromium preparations

Solutions of Cr_{aq}^{2+} and L^1Cr^{2+} were prepared by Zn/Hg reduction of their respective 3+ ions under argon. $Cr_{aq}OO^{2+}$ was prepared by injecting 5 mM Cr_{aq}^{2+} into ice-cold, oxygen-saturated solutions of 0.10 M $HClO_4$ containing ~0.2 M methanol, and standardized spectrophotometrically ($\varepsilon_{293\ nm} = 3.0 \times 10^3\ M^{-1}\ cm^{-1}$). Total Cr concentrations under 0.2 mM typically give yields greater than 80%. These solutions were used immediately. $L^1Cr(H_2O)OO^{2+}$ was prepared by a similar procedure, but without the methanol. Owing to their greater stability, solutions of this complex were used over several hours.[11]

Preparation of $Cr_{aq}OOH^{2+}$

Solutions of $Cr_{aq}OO^{2+}$ were reduced to the hydroperoxo- by approximately 10 % excess $Ru(NH_3)_6^{2+}$, which was prepared by Zn/Hg reduction of the 3+ ion under argon. The reaction was rapid and complete upon mixing. The absence of the characteristic $Cr_{aq}OO^{2+}$ spectrum confirmed complete conversion of the superoxo- into $Cr_{aq}OOH^{2+}$.

Preparation of $Rh(NH_3)_4(H_2O)OOH^{2+}$, $L^1Rh(H_2O)OOH^{2+}$, and $L^2Rh(H_2O)OOH^{2+}$

~0.5-1 mM solutions of the appropriate RhH were saturated with O_2, and their pH was then adjusted to 9–11 using $NH_{3\ (aq)}$. These solutions were then re-acidifed,

generating the desired hydroperoxide. Yields ~75% are typical. The deuterated analogs were prepared in the same way, only replacing H_2O with D_2O. A second approach, photolysis of the Rh-H bond under an O_2 atmosphere, was avoided due to the presence of reactive impurities such as the initial Rh-H as well as RhOO along with the hydroperoxide in the reaction mixture.[12]

Preparation of $L^2Co(H_2O)OOH^{2+}$

A 10 mg sample of $[L^2Co(H_2O)_2](CF_3SO_3)_2$ was dissolved in 5-6 mL argon saturated 0.05 M $HClO_4$. To this solution is added an equimolar amount of $Ru(NH_3)_6^{2+}$, prepared by Zn/Hg reduction of its 3+ ion under argon. This mixture is placed on ice, then transferred to a beaker and vigorously sparged with oxygen for ~ 15 min, during which time a color change from pink to light green is observed. In order to remove $Ru(NH_3)_6^{3+}$ and $L^2Co_{aq}^{3+}$ byproducts, this mixture can be further purified by ion exchange chromatography on SP-Sephadex C-25 resin that has been pre-treated with HCl/H_2O_2, however, omitting this step did not have an effect on the reactivity, but did on the resulting spectrum, since the $L^2Co_{aq}^{3+}$ and $Ru(NH_3)_6^{3+}$ present as byproducts significantly contribute to the spectrum. Pre-treatment of the resin with H_2O_2 is crucial, if it is omitted the compound decomposes on the column.[13,14]

Preparation of $Cr^{IV}{}_{aq}O^{2+}$

A solution of Cr_{aq}^{2+} was prepared by Zn/Hg reduction of its respective 3+ ion under argon. Chromyl ion was prepared by injecting 5 mM Cr_{aq}^{2+} into a standard I cm cuvette containing 2.8 mL of air-saturated 0.10 M $HClO_4$. $Cr^{IV}{}_{aq}O^{2+}$ was then converted into $Cr_{aq}OO^{2+}$ using methanol, which was then standardized spectrophotometrically ($\varepsilon_{293\ nm} = 3.0 \times 10^3\ M^{-1}\ cm^{-1}$). Typically yields of $Cr^{IV}{}_{aq}O^{2+}$ were 0.04 -0.05 mM with 0.01-0.02 mM $Cr_{aq}OO^{2+}$ as a side product when using total Cr concentrations of ~0.15 mM. These solutions were used immediately after preparation.[15]

[14]aneN_4 and $[Ru(NH_3)_6](Cl)_3$ were purchased from commercial sources and used without further purification. [$L^1Cr(Cl)_2$]Cl, [$L^1Rh(Cl)_2$]Cl, $[L^2Rh(H_2O)H](CF_3SO_3)_2$, $[Rh(NH_3)_5H](SO_4)$, and *meso*-Me_6-[14]aneN_4 were available from our previous work.

Kinetic measurements were carried out by conventional UV-vis spectrophotometry using a Shimadzu 3101 PC spectrophotometer, thermostated at 25 ± 0.2 °C. There was no batch dependence on reacti on rates. Most of the experiments were carried out using manual mixing, but when fast mixing was required, a thermostated OLIS RSM-1000 stopped-flow spectrophotometer was used. Oxygen evolution was measured with a YSI model 5300 biological oxygen monitor, thermostated at 25 ± 1 °C.

Results

The reaction of $LRh(H_2O)OOH^{2+}$ with $LCr(H_2O)OO^{2+}$

Superoxochromium complexes with both aqua and macrocyclic ligands oxidize hydroperoxorhodium ions to their corresponding superoxorhodium complex, themselves being reduced to hydroperoxochromium. Initial rates were used to study the kinetics of the reaction of hydroperoxorhodium ions with superoxochromium ions. Full time-courses were not used since all reactions of interest suffer from slower secondary reactions, in some cases between products and starting materials, as well as the inherent instability of the compounds towards decomposition over the longer timescales necessary to study the full timecourse. These reactions were monitored at 270 nm, where the growth in absorbance due to the formation of superoxorhodium ion, which is the dominant spectral feature, causing a net $\Delta\varepsilon = 7 \times 10^3\ M^{-1}\ cm^{-1}$. The hydroperoxochromium ion products absorb only weakly in the same regions as the superoxorhodium products, contributing little to the reaction

mixture spectrum and remaining essentially invisible. However, in the case where $L^1Cr(H_2O)OO^{2+}$ was used as oxidant, the decrease in its distinctive spectrum at ~630 nm can be used to confirm qualitatively that the superoxochromium was being consumed during the course of the reaction. Representative spectra are shown in Fig. 1 and 2.

From the observed absorbance change and known $\Delta\varepsilon$, the stoichiometry was shown to be 1Cr:1Rh. Even in reactions measured for the full timecourse, the stoichiometry appeared to be nearly 1:1, but endpoint absorbances were decidedly less reliable due to secondary reactions and decomposition of the products and starting material over longer periods of time. The initial rates responded to the concentrations of both species and did not diverge depending on the identity of the reagent in excess, or under ~1:1 concentrations. This confirms the stoichiometry.

Plots of initial rate, as determined from the absorbance change, v_i vs. the product of $[LCr(H_2O)OO^{2+}]$ x $[LRh(H_2O)OOH^{2+}]$ concentrations are linear, with a slope equal to the rate constant. Plots of the log (v_i) vs. log (product of concentration) are linear with slopes of 1, confirming the orders of the reagents as well as the form of the rate law. A *k*H/*k*D kinetic isotope effect of 2.9 was found for the oxidation of $Rh(NH_3)_4(H_2O)OOH^{2+}$ and its deuterated analog $Rh(NH_3)_4(D_2O)OOD^{2+}$ by $Cr(D_2O)_5OO^{2+}$ in D_2O. The significance of this will be discussed later. There was no effect on reaction rate due to the mixing order of the reagents.

$$v_i = k[LCr(H_2O)OO^{2+}][LRh(H_2O)OOH^{2+}] \qquad (4)$$

The rates of reaction increased as a function of the ionic strength. This is in accordance with the Debye-Hückel equation, and is consistent with the reaction of two positively charged species, where z_a and z_b represent the charges of the

individual species, μ the ionic strength, k_{ref} the rate-constant at zero ionic strength, and the constant $A = 0.509$ for aqueous solutions.

$$\log k = \log k_{ref} + \frac{2z_a z_b A\mu^{1/2}}{1+\mu^{1/2}} \qquad (5)$$

The position of the equilibrium can only be examined in the reactions between $Cr_{aq}OO^{2+}$ with $Rh(NH_3)_4(H_2O)OOH^{2+}$ and $L^2Rh(H_2O)OOH^{2+}$. As both products can be prepared and are relatively stable, the reverse reaction between these superoxorhodium ions and $Cr_{aq}OOH^{2+}$ can be studied independently. No reverse reaction was observed, except for a slight Abs. increase at 270 nm due to decomposition of the hydroperoxochromium ion into $HCrO_4^-$ over 10-30 min ($Cr_{aq}OOH^{2+}$ decomposition has $t_{½}$ ~ 15 min. in 0.1 M $HClO_4$).[16] The presence of nearly quantitative amounts of $HCrO_4^-$ in the product spectrum confirms that little or no $Cr_{aq}OO^{2+}$ was being formed. Also, there were no obvious changes in the spectrum of superoxorhodium ion, nor was there any formation of an appreciable amount of hydroperoxorhodium ion.

$$Cr_{aq}OO^{2+} + LRh(H_2O)OOH^{2+} = Cr_{aq}OOH^{2+} + LRh(H_2O)OO^{2+} \quad K_6 \qquad (6)$$

The decomposition of $Cr_{aq}OOH^{2+}$ allows us to place a conservative limit of <1 M^{-1} s^{-1} as the maximum rate constant for the reverse reaction, corresponding to K_6 values >46 for $Rh(NH_3)_4(H_2O)OOH^{2+}$ and K_6 >17 for $L^2Rh(H_2O)OOH^{2+}$. When $L^1Cr(H_2O)OO^{2+}$ was used as the oxidant, its corresponding hydroperoxometal complex decomposes rapidly, making the determination of the equilibrium position of $L^1Cr(H_2O)OO^{2+}$ with $LRh(H_2O)OOH^{2+}$ impossible, since the equilibrium observed for the first step is affected by concentration changes in secondary steps.

Mn_{aq}^{2+} did not affect the initial rate of the reaction, which established that the chromyl ion, and possibly other strong oxidants, do not play a role in the initial hydrogen atom transfer to $Cr_{aq}OO^{2+}$. Chromyl is a powerful oxidant that abstracts hydrogen atoms from a variety of substrates, and is a known product in $Cr_{aq}OO^{2+}$ decomposition.

$$Cr_{aq}OO^{2+} = Cr_{aq}^{2+} + O_2 \quad (7)$$

$$2Cr_{aq}^{2+} + Cr_{aq}OO^{2+} + 2H^+ \rightarrow Cr^{IV}{}_{aq}O^{2+} + 2Cr_{aq}^{3+} \quad (8)$$

The reaction of chromyl ion with $Rh(NH_3)_4(D_2O)OOD^{2+}$ will be discussed later in this chapter. Large amounts of chromyl ion from $Cr_{aq}OO^{2+}$ decomposition should be prevented by the presence of MeOH in oxygen-saturated reaction solutions, but a low steady-state concentration of $Cr^{IV}{}_{aq}O^{2+}$ will remain.

$$Cr^{IV}{}_{aq}O^{2+} + CH_3OH + H^+ \rightarrow Cr_{aq}^{2+} + CH_2O + H^+ \quad (9)$$

$$Cr_{aq}^{2+} + O_2 \rightarrow Cr_{aq}OO^{2+} \quad (10)$$

It is known that chromyl ion oxidizes Mn_{aq}^{2+} and is removed from the system as unreactive Cr_{aq}^{3+}.[17]

$$Cr^{IV}{}_{aq}O^{2+} + Mn_{aq}^{2+} + 2H^+ \rightarrow Cr_{aq}^{3+} + Mn_{aq}^{3+} \quad (11)$$

The initial rate was independent of the presence or concentration of Mn_{aq}^{2+} up to 7 mM. This shows chromyl ion plays no role in the initial reactivity of $Cr_{aq}OO^{2+}$. By

the same reasoning, other strongly oxidizing high-valent metal species, such as Rh^{IV}, are also likely not participating in the initial reaction. This is not guaranteed, as the reaction of Rh^{IV} with Mn_{aq}^{2+} has not been observed, but such a reaction should be exorgonic and rapid.[12]

The initial rates also did not vary when up to 0.1 M hydrogen peroxide is included in the reaction mixture, or when oxygen was removed from the reaction mixture. These were tests for the involvement of reduced metal ions, such as Rh_{aq}^{2+} and Cr_{aq}^{2+}, in the chemistry. Hydrogen peroxide reacts quickly (3×10^4 M^{-1} s^{-1} for Cr_{aq}^{2+}) [18] with reduced metal ions via a Fenton-like mechanism, generating unreactive M^{III} and the •OH radical.

$$M^{II} + H_2O_2 \rightarrow M^{III}(OH) + \bullet OH \qquad (12)$$

If reduced metal ions play an important role in the chemistry, it is expected that removing them via the Fenton reaction and replacing them with the powerful hydroxyl radical would affect the kinetics as well as the products generated.

Similarly, if reduced metal ions were being generated in the system they should be extremely sensitive to oxygen concentration. The equilibrium in eq 7 lies far towards the reactant, but removing O_2 from the reaction vessel encourages the dissociation of $Cr_{aq}OO^{2+}$ and subsequent formation of chromyl ion through eq 8. As such, $Cr_{aq}OO^{2+}$ solutions could not be exhaustively deaerated without increasing the concentration of $Cr^{IV}{}_{aq}O^{2+}$. $L^1Cr(H_2O)OO^{2+}$ solutions did not suffer from this complication and could be saturated with Ar without rapidly decomposing the superoxometal complex or generating other reactive intermediates. These solutions showed the same reactivity towards $LRh(H_2O)OOH^{2+}$ as those under O_2. The insensitivity of the reaction towards hydrogen peroxide and oxygen concentration supports the absence of reduced metal species in the chemistry.

Oxygen evolution from the system was also monitored as a function of time. Due to the limits in the oxygen-monitoring system, it is difficult to measure the fast initial rates (< 45 s) of oxygen evolution that would correspond with the initial rates of the reaction measured spectrophotometrically. However, during the later part of the reaction, no additional oxygen evolution was observed apart from what is normally seen in known hydroperoxo- and superoxometal complex decomposition. This evidence supports cleaving the OO-H bond as opposed to the O-OH bond, which would generate a strongly oxidizing high-valent metal-oxo species, analogous to hydroxyl radical in the Fenton reaction, and also oxygen. This would be the case for a metal analog to the Haber-Weiss reaction, where superoxide (hydroperoxyl radical) oxidizes hydrogen peroxide to a hydroxyl radical and oxygen, itself being reduced to water, as shown in eq 3. The observed stoichiometry and products are inconsistent with this, and the real Haber-Weiss reaction is slow, at best, and most likely always catalyzed by a metal ion, such as $Fe^{2/3+}$ in the modified Haber-Weiss scheme. [1,19]

$$Fe^{3+} + HO_2 \rightarrow Fe^{2+} + H^+ + O_2 \qquad (13)$$

$$Fe^{2+} + H_2O_2 \rightarrow Fe^{3+} + \bullet OH + {}^-OH \qquad (14)$$

No acid effect was observed over a low range of acid concentrations, 0.02-~0.04 M. Hydroperoxometal species are most stable at low acid concentrations (< 0.01 M), whereas superoxochromium species tend to be most stable at higher acid concentrations (≥ 0.1 M). This severely limits the acid concentration range that these reactions can be studied in, and 0.02 M was chosen as a compromise that allowed relatively long lifetimes for both species and virtually no change due to decomposition during the initial period of the reactions. However, due to the limited

pH range of stabilities of these compounds, results are not systematic enough to rule out acid effects outside this small range of acid concentrations.

The reaction of $L^2Co(H_2O)OOH^{2+}$ with $Cr_{aq}OO^{2+}$

The aquasuperoxochromium ion is also capable of oxidizing the macrocyclic hydroperoxocobalt complex $L^2Co(H_2O)OOH^{2+}$. Unlike the analogous reaction with hydroperoxorhodium ions, the full timecourse for $L^2Co(H_2O)OOH^{2+}$ oxidation can be analyzed. This is due in part to the faster rate of the reaction, which makes the slower secondary reactions less important to the initial absorbance change observed. Also, $L^2Co(H_2O)OO^{2+}$ and $L^2Co_{aq}^{2+}$ are rapidly trapped, generating unreactive $L^2Co_{aq}^{3+}$ and preventing any further side reactions. Unfortunately the slower reaction of $Cr(D_2O)_5OO^{2+}$ with $L^2Co(D_2O)OOD^{2+}$ in D_2O was not as well behaved as the H_2O case, with a slow linear decrease in absorbance that interfered with the data analysis for the faster initial reaction. It is not clear which subsequent or side reactions became more important in D_2O, or if a parallel path operates in the deuterated system, only that the overall rate slowed down significantly, on the order of ~2-3 fold.

The plot of k_{obs} vs. $2[L^2Co(H_2O)OOH^{2+}]_{avg}$ and $[Cr_{aq}OO^{2+}]_{avg}$ is shown in Figure 7. It is linear with a slope of $k = 130\ M^{-1}\ s^{-1}$ in 0.05 M $HClO_4$. In reactions carried out with excess $Cr_{aq}OO^{2+}$, the plot of k_{obs} vs. $[Cr_{aq}OO^{2+}]_{avg}$ falls on the same line as the points for $2[L^2Co(H_2O)OOH^{2+}]_{avg}$ in excess Co, confirming the 2Cr:1Co stoichiometry, and giving the following rate law:

$$-\frac{1}{2}\frac{d[Cr_{aq}OO^{2+}]}{dt} = -\frac{d[L^2Co(H_2O)OOH^{2+}]}{dt} = k[Cr_{aq}OO^{2+}][L^2Co(H_2O)OOH^{2+}] \qquad (15)$$

The measured absorbance change is also consistent with a stoichiometry of 2Cr: 1Co. In reactions carried out under ~1:1 concentration conditions, the fit to the

2^{nd}-order eq 16 yielded rate constants in the range 120-160 M^{-1} s^{-1}, in good agreement with the value obtained from the plot of k_{obs} vs. average excess reagent concentration.

$$Abs_t = \frac{Abs_\infty + \{Abs_0(1-\frac{[A]_0}{[B]_0}) - Abs_\infty\}e^{-k\Delta_0 t}}{1-\frac{[A]_0}{[B]_0}e^{-k\Delta_0 t}} \quad (16)$$

Following Abs_t at 295nm, where $[A]_0$ represents the limiting reagents initial concentration and $[B]_0$ represents the excess reagents initial concentration. Δ_0 represents the difference in initial concentration = $a[B]_0$ - $b[A]_0$, using coefficients a and b to adjust for the proper stoichiometry.

The results suggest an initial oxidation produces aquahydroperoxochromium and the unstable superoxocobalt product $L^2Co(H_2O)OO^{2+}$, which undergoes rapid Co-O bond homolysis generating reducing $L^2Co_{aq}^{2+}$ and oxygen. The cobalt(II) species is rapidly trapped by a second equivalent of $Cr_{aq}OO^{2+}$, yielding another $Cr_{aq}OOH^{2+}$ and $L^2Co_{aq}^{3+}$, which can be seen as a shoulder in the product spectrum around 380 nm. This reaction is summarized in eq 17-20, including the known rate constants for the subsequent reactions.[10,20,21]

$$Cr_{aq}OO^{2+} + L^2Co(H_2O)OOH^{2+} \rightarrow Cr_{aq}OOH^{2+} + L^2Co(H_2O)OO^{2+} \quad k_{17} = 130\ M^{-1}\ s^{-1} \quad (17)$$

$$L^2Co(H_2O)OO^{2+} = L^2Co_{aq}^{2+} + O_2 \quad k_{18} = 5 \times 10^6\ s^{-1},\ k_{-18}\ 2 \times 10^4\ M^{-1}\ s^{-1} \quad (18)$$

$$Cr_{aq}OO^{2+} + L^2Co_{aq}^{2+} + H^+ \rightarrow Cr_{aq}OOH^{2+} + L^2Co_{aq}^{3+} \quad k_{19} \sim 10^7\ M^{-1}\ s^{-1} \quad (19)$$

net: $2Cr_{aq}OO^{2+} + L^2Co(H_2O)OOH^{2+} + H^+ \rightarrow 2Cr_{aq}OOH^{2+} + L^2Co_{aq}^{3+}$ (20)

The reaction of $Rh(NH_3)_4(D_2O)OOD^{2+}$ with $Cr^{IV}(D_2O)_5O^{2+}$

The chromyl ion was found to rapidly oxidize the tetrammine hydroperoxorhodium ion to its corresponding superoxide, itself being reduced to the spectroscopically invisible Cr^{3+} aqua ion. At 25 °C and in 0.1 M $DClO_4$ in D_2O, the plot of k_{obs} vs. average chromyl ion concentration is linear and passes through the origin, with the slope equal to the rate constant 2 x 10^3 M^{-1} s^{-1}, as seen in Fig. 7. When the reaction was carried out in H_2O it was complete in mixing time, generating a quantitative yield of superoxorhodium product. The slower secondary reaction of $Cr(D_2O)_5OO^{2+}$ with excess $Rh(NH_3)_4(D_2O)OOD^{2+}$ was observed when a large excess of Rh was used and significant amounts of $Cr(D_2O)_5OO^{2+}$ was generated during chromyl preparation. Even in water at 5 °C, more than 5 half-lives were complete in <10 s, placing a conservative estimate on the rate constant of >10^4 M^{-1} s^{-1} in H_2O, and a correspondingly large kie >5. Rapid-scanning stopped-flow studies at ~10 °C and 5 °C repeat-scan studies showed no formation of any colored intermediates, but only the conversion of $Rh(NH_3)_4(D_2O)OOD^{2+}$ into $Rh(NH_3)_4(D_2O)OO^{2+}$.

Discussion

Chromyl ion and the superoxochromium ions $Cr_{aq}OO^{2+}$ and $L^1Cr(H_2O)OO^{2+}$ are powerful oxidants, and they oxidize hydroperoxorhodium and hydroperoxocobalt complexes completely, that is, the equilibrium lies far to the right in these reactions. However, the relative instability and subsequent secondary reactions when $L^1Cr(H_2O)OOH^{2+}$ and $L^2Co(H_2O)OO^{2+}$ are produced make determining the precise equilibrium position of the first step impossible, although it is clear that the overall process proceeds to completion. This is consistent with what is known of the redox

potentials of the respective species. Chromyl ion is the strongest oxidant and consequently the most reactive species in hydrogen atom transfer (HAT), followed by the $Cr_{aq}OO^{2+}$ and $L^1Cr(H_2O)OO^{2+}$. This is expected from what has been observed in previous reactions of chromyl and superoxochromium ions, such as the oxidations of $L^1Rh(H_2O)H^{2+}$ and substituted phenol, with rate constants $>10^3$ larger for chromyl ion. Many hydrogen atom transfer reactions of these ions are summarized in Table 1.

There is a significant *k*H/*k*D kinetic isotope effect (kie) for the oxidations of $Rh(NH_3)_4(H_2O)OOH^{2+}$ and $L^2Co(H_2O)OOH^{2+}$ by $Cr_{aq}OO^{2+}$, of 2.9 and ~2-3 respectively. The chromyl ions oxidation of $Rh(NH_3)_4(D_2O)OOD^{2+}$ has a kie >5. It is reasonable to expect a significant kie if hydrogen atom transfer from hydroperoxometal to chromium oxidant is the rate limiting step. In other hydrogen atom transfer reactions with superoxochromium and chromyl as oxidants, significant kie values are reported, and these values are summarized in Table 1. The kie values strongly suggest that the breaking of the O-H or O-D bond is important to the oxidation of hydroperoxometal ions either by a hydrogen atom transfer or proton coupled electron transfer mechanism. A rate limiting electron transfer, followed by protonation, would not produce a significant kie.

The reactions studied are not particularly fast, especially when the superoxochromium ions are oxidants, implying that there is a significant kinetic barrier to the reaction. It is reasonable that this barrier involves cleaving the O-H bond of the hydroperoxometal ion. If hydrogen atom transfer is the mechanism, the kinetic barrier and consequently the rate of the reaction will be largely determined by the BDE of the reductants element-H bond.[22-24] This can be seen in Table 1., comparing the rate of hydrogen atom abstraction by $Cr_{aq}OO^{2+}$ from the O-H bond in a substituted phenol ArOH, the Rh-H bond in $Rh(NH_3)_4(H_2O)H^{2+}$, and the RhOO-H

bond in $Rh(NH_3)_4(H_2O)OOH^{2+}$. The slowest (1.24 $M^{-1} s^{-1}$) hydrogen atom abstraction by $Cr_{aq}OO^{2+}$ is from the ArO-H bond in the substituted phenol is consistent with its relatively high O-H BDE of ~80 kcal mol^{-1}. On the other hand, a fast 129 $M^{-1} s^{-1}$ rate constant is observed when abstracting hydrogen atom from the weaker Rh-H bond, with a BDE ~60 kcal mol^{-1}.[25] One can interpolate between these two points, knowing our rate constants are in the range of 46 $M^{-1} s^{-1}$ to 17 $M^{-1} s^{-1}$ with $Cr_{aq}OO^{2+}$ and $LRh(H_2O)OOH^{2+}$. Assuming relatively similar self-exchange rate constants between the species being compared, the BDE for LRhOO-H is likely somewhere between 60 and 80 kcal mol^{-1}. This estimate suggests that the hydroperoxorhodium O-H bond is significantly lower in energy than the HOO-H bond in hydrogen peroxide, which is 88 kcal mol^{-1}, and typical ROO-H bonds between 85-90 kcal mol^{-1}.[26]

The respective ligands surrounding the superoxo- and hydroperoxometal complexes play only a small role in determining their reactivity. This is consistent with the chemistry taking place on the coordinated oxygen derivatives, more or less independent of the rest of the coordination sphere. This trend is reinforced by comparison to other known rate constants for HAT reactions involving these complexes in Table 1. The superoxo and hydroperoxo ligands appear to be relatively insulated from substituent induced steric and electronic effects. Sterics greatly influence the rate of hydrogen atom transfer from Rh-H. When two macrocyclic species react by abstracting H-atoms bound directly to the metal, such as $L^1Cr(H_2O)OO^{2+}$ and $L^1Rh(H_2O)H^{2+}$, the rate of the reaction is too slow to measure; but $Cr_{aq}OO^{2+}$ readily oxidizes $L^1Rh(H_2O)H^{2+}$. This is not seen in the analogous superoxo-hydroperoxo reaction, where $L^1Cr(H_2O)OO^{2+}$ oxidizes $L^1Rh(H_2O)OOH^{2+}$ slightly *faster* than $Cr_{aq}OO^{2+}$, 36 $M^{-1} s^{-1}$ compared to 23 $M^{-1} s^{-1}$.

The insulation from electronic effects is similar. $Cr_{aq}OO^{2+}$ and $L^1Cr(H_2O)OO^{2+}$ oxidize the hydroperoxorhodium series with rate constants that are closely grouped

regardless of the differing electron donating effects of the ancillary aq and cyclam ligands. Also, little difference is seen in the rate constants for L^1-, L^2- and $(NH_3)_4$-$Rh(H_2O)OOH^{2+}$ oxidation by $Cr_{aq}OO^{2+}$, showing no significant trend in electronics of the reductant. The lack of electronic effects is again indicative of the decreasing influence of ancillary ligands on the chemistry of hydroperoxo- and superoxometal complexes.

Although it is clear that the identity of the metal atom is important to the thermodynamics in the reactions studied, it has relatively little effect on the rates of these reactions. The measured rate constant for the reaction between $Cr_{aq}OO^{2+}$ and $L^2Co(H_2O)OOH^{2+}$ increase only by an order of magnitude from that of the analogous reaction with $L^2Rh(H_2O)OOH^{2+}$, suggesting changes in reactivity by moving up or down the periodic table from Co to Rh are not tremendously large in this type of reaction. This is reasonable, since all the complexes prepared are relatively long lived, as well as having inert coordination spheres. These kinetic factors, combined with very large O_2 and HO_2^- binding constants for all species studied, means the complexes are all, to varying degrees, stable.

Conclusion

Hydroperoxo complexes of rhodium and cobalt can be completely oxidized by the chromyl ion and by superoxochromium ions in aqueous acid. The significant kie and rate laws support a hydrogen atom abstraction from the hydroperoxometal complex, generating the corresponding superoxometal complex as product. The rates correlate with the relative redox power of the oxidants, as well as the BDEs of element-H bonds involved in the hydrogen atom transfer. Substituent and ligand effects are relatively small when compared to other hydrogen atom transfer reactions with the same oxidants.

Table 1. A summary of hydrogen-atom transfer reactions.

oxidant	reductant	k (M^{-1} s^{-1})	kie	Ref.
$Cr_{aq}OO^{2+}$	$Rh(NH_3)_4(H_2O)OOH^{2+}$	46 ± 2	2.9	*a*
$Cr_{aq}OO^{2+}$	$L^1Rh(H_2O)OOH^{2+}$	23 ± 1		*a*
$Cr_{aq}OO^{2+}$	$L^2Rh(H_2O)OOH^{2+}$	17 ± 1		*a*
$Cr_{aq}OO^{2+}$	$L^2Co(H_2O)OOH^{2+}$	130 ± 20	~2-3	*a*
$Cr_{aq}OO^{2+}$	$Rh(NH_3)_4(H_2O)H^{2+}$	135		*b*
$Cr_{aq}OO^{2+}$	$L^1(H_2O)RhH^{2+}$	129	7.6	*b*
$Cr_{aq}OO^{2+}$	$L^2(H_2O)RhH^{2+}$	24		*b*
$Cr_{aq}OO^{2+}$	ArOH[f]	1.24	~12	*b*
$Cr^{IV}{}_{aq}O^{2+}$	ArOH[f]	470	14.7	*c*
$Cr^{IV}{}_{aq}O^{2+}$	$Cr_{aq}OOH^{2+}$	1340	5.0	*c*
$Cr^{IV}{}_{aq}O^{2+}$	$L^1(H_2O)RhH^{2+}$	1.0×10^4	3.7	*d*
$Cr^{IV}{}_{aq}O^{2+}$	$L^2(H_2O)RhH^{2+}$	1100	3.3	*d*
$Cr^{IV}{}_{aq}O^{2+}$	$Rh(NH_3)_4(D_2O)OOD^{2+}$	$2 \pm 0.2 \times 10^3$	>5	*a*
$Cr^{IV}{}_{aq}O^{2+}$	H_2O_2	191	3.6	*e*
$L^1Cr(H_2O)OO^{2+}$	$Rh(NH_3)_4(H_2O)OOH^{2+}$	19 ± 1		*a*
$L^1Cr(H_2O)OO^{2+}$	$L^1Rh(H_2O)OOH^{2+}$	36 ± 2		*a*
$L^1Cr(H_2O)OO^{2+}$	$Rh(NH_3)_4(H_2O)H^{2+}$	3		*b*
$L^1Cr(H_2O)OO^{2+}$	$L^1(H_2O)RhH^{2+}$	<1		*b*
$Rh(NH_3)_4(H_2O)OO^{2+}$	$Cr_{aq}OOH^{2+}$	<1		*a*
$L^2Rh(H_2O)OO^{2+}$	$Cr_{aq}OOH^{2+}$	<1		*a*
$Rh(NH_3)_4(H_2O)OO^{2+}$	$Rh(NH_3)_4(H_2O)H^{2+}$	33		*b*

a This work. *b* Ref. 27. *c* Ref. 28. *c* Ref. 16. *d* Ref. 30. *e* Ref. 31. *f* ArOH is phenol 2-methyl-2-(4-hydroxy-3,5-di-*tert*-butylphenyl)propylammonium chloride.

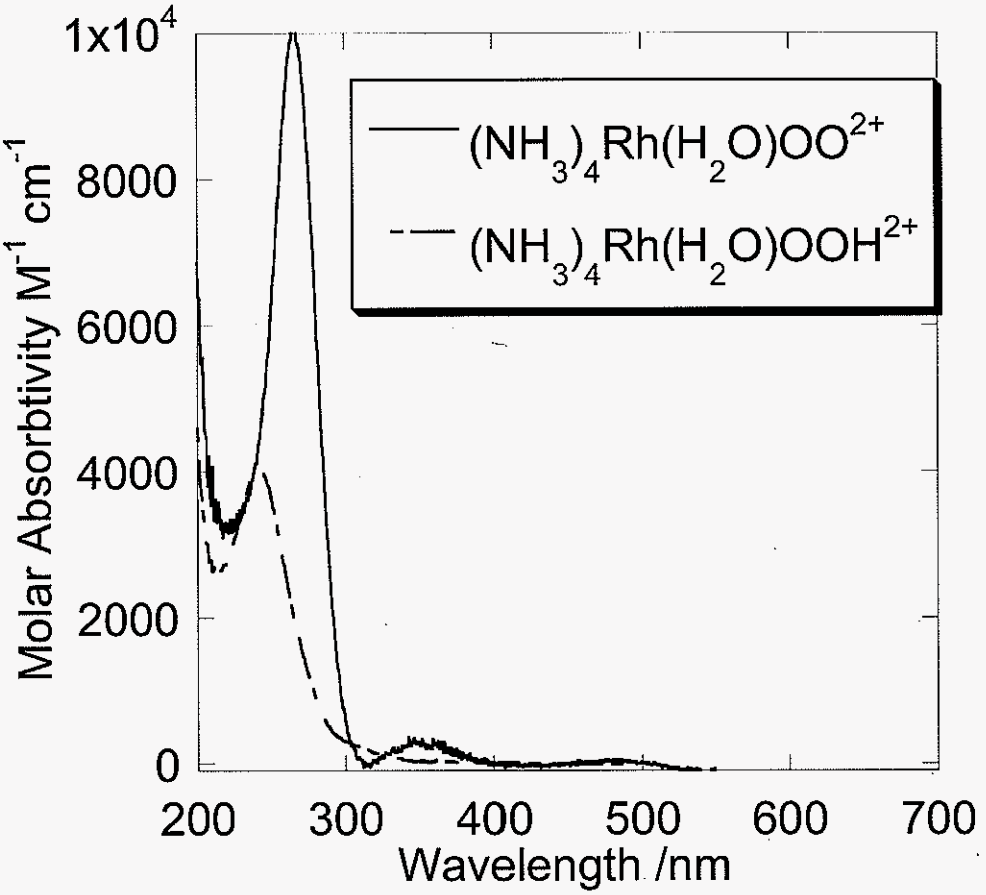

Figure 1. Representative UV-vis spectra of hydroperoxo- and superoxorhodium ions in aqueous acid.

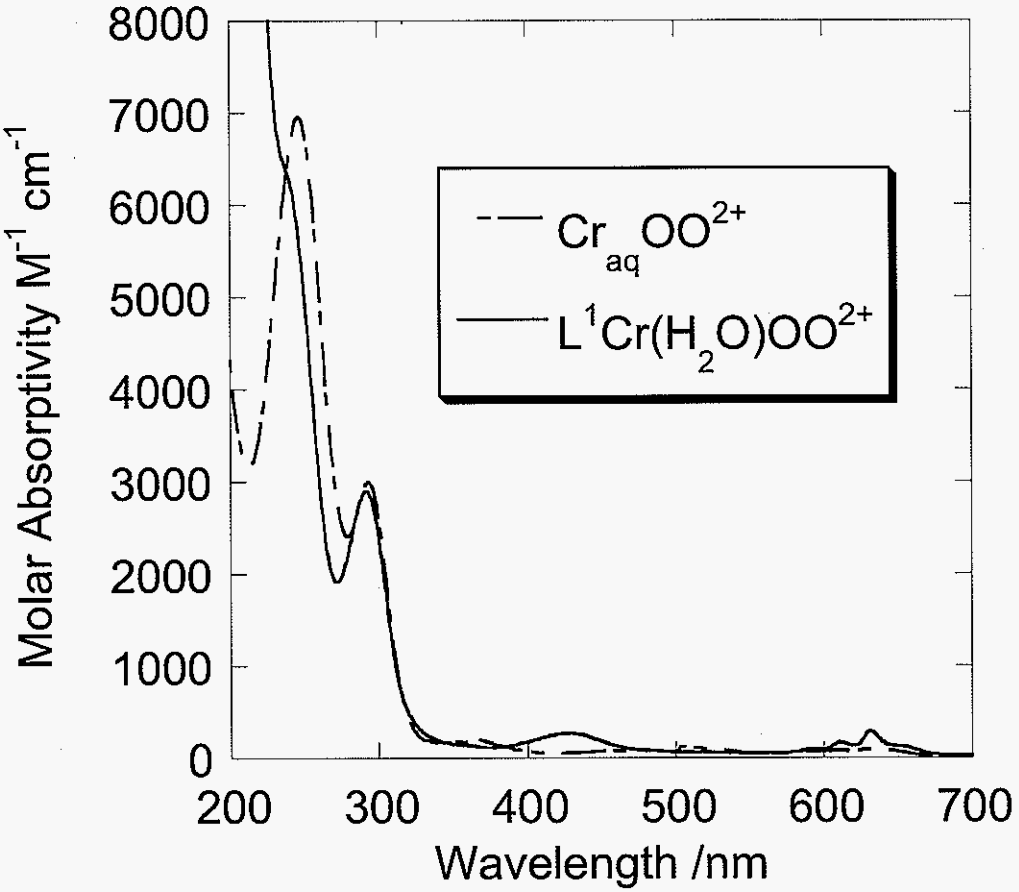

Figure 2. Representative UV-vis spectra of superoxochromium ions in aqueous acid.

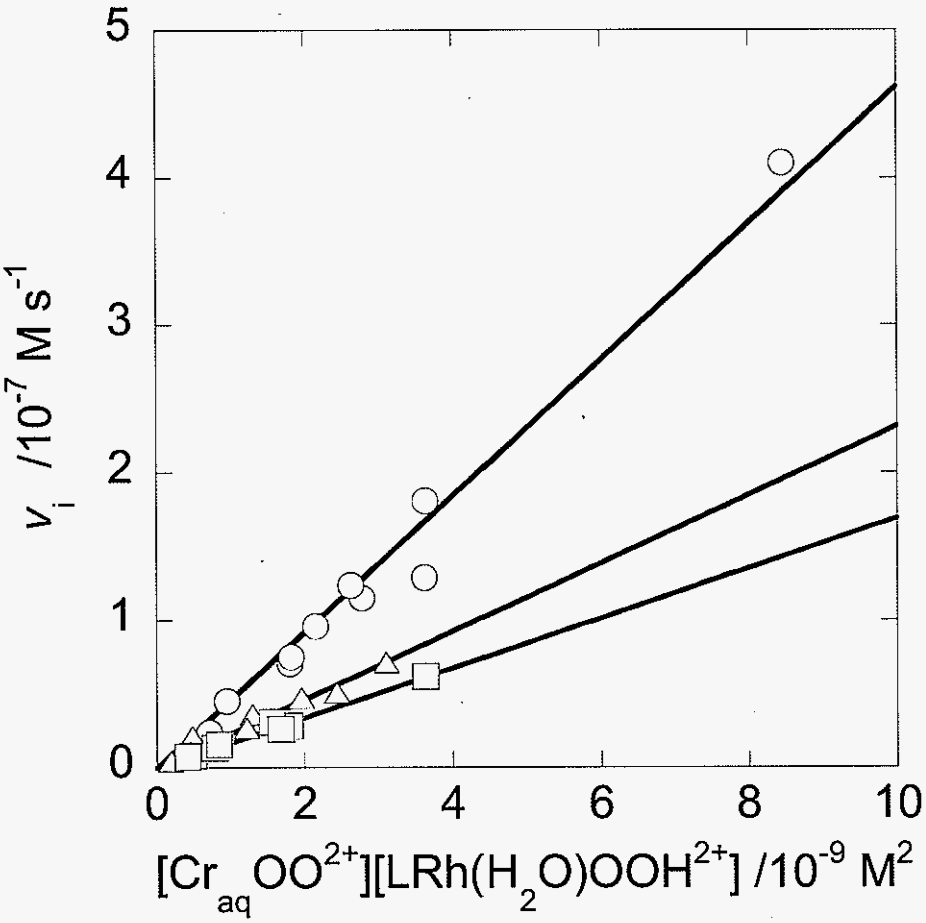

Figure 3. Initial rate as a function of ([$Cr_{aq}OO^{2+}$] x [$LRh(H_2O)OOH^{2+}$]) at 25 °C. Slope = k = 46 ± 2 L = $(NH_3)_4$ = ○, 23 ± 1 L = L^1 = Δ, 17 ± 1 M^{-1} s^{-1} L = L^2 = □.
Conditions: [$Cr_{aq}OO^{2+}$] = 7 x 10^{-6} – 1.6 x 10^{-4} M; [$Rh(NH_3)_4(H_2O)OOH^{2+}$] = 1.4 x 10^{-5} – 1.4 x 10^{-4} M; [$L^1Rh(H_2O)OOH^{2+}$] = 1.4 x 10^{-5} – 1.8 x 10^{-4} M; [$L^2Rh(H_2O)OOH^{2+}$] = 1.2 x 10^{-5} – 1.6 x 10^{-4} M; [$HClO_4$] = 0.02 M = μ.

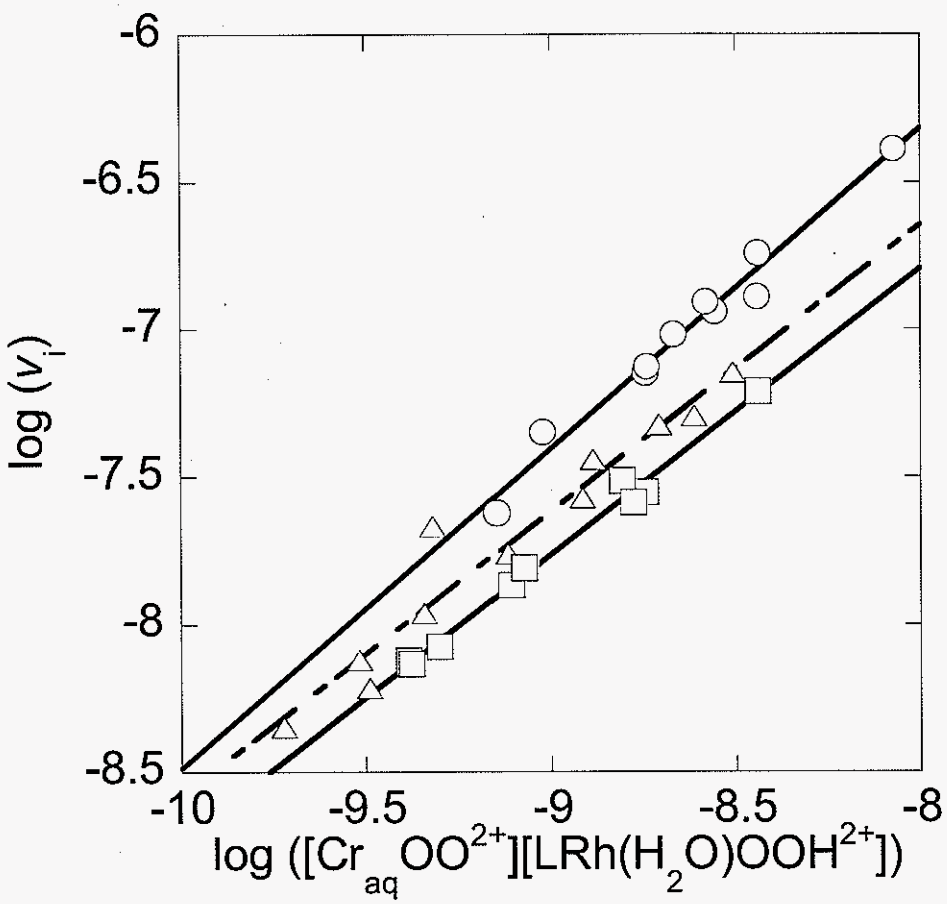

Figure 4. Log (Initial rate) as a function of the log ([$Cr_{aq}OO^{2+}$] x [$LRh(H_2O)OOH^{2+}$]). Slope = 1 ± .04.

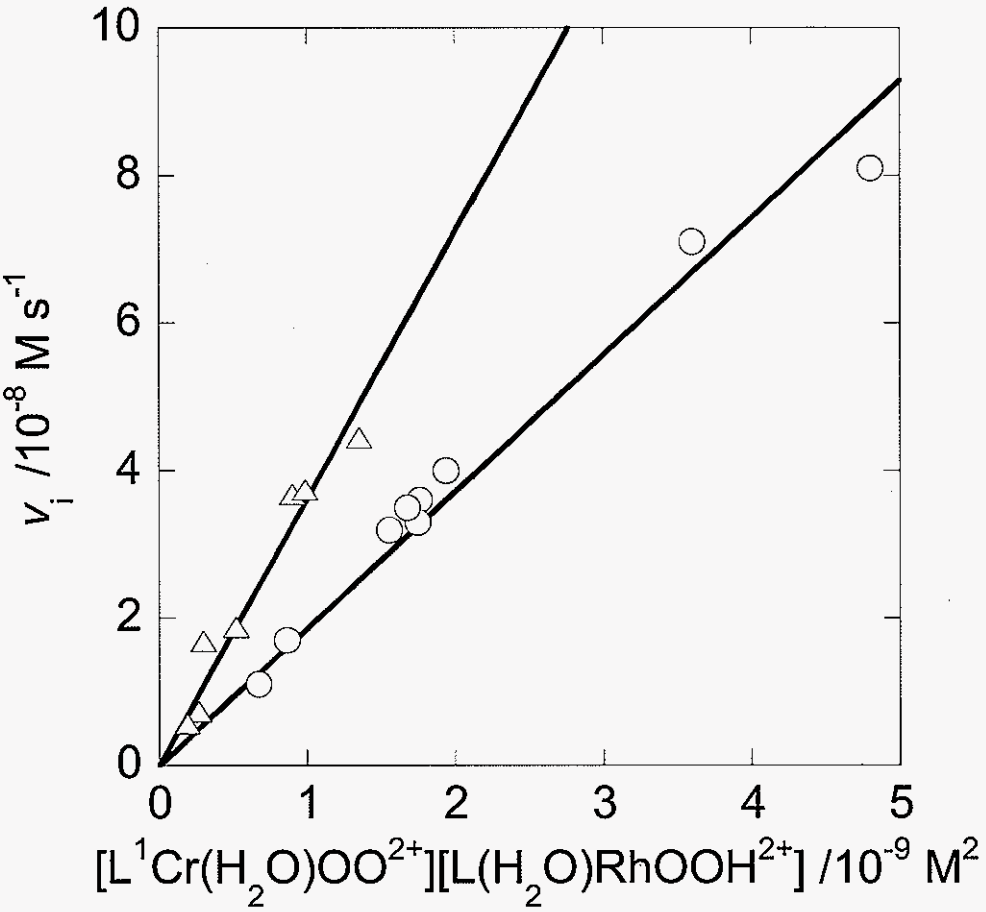

Figure 5. Initial rate as a function of ([$L^1Cr(H_2O)OO^{2+}$] x [$LRh(H_2O)OOH^{2+}$]) at 25 °C Slope = k = 19 ± 1 L = $(NH_3)_4$, = ○ 36 ± 2 M^{-1} s^{-1} L = L^1 = Δ Conditions: [$L^1Cr(H_2O)OO^{2+}$] = 6 x 10^{-6}–8.2 x 10^{-4} M; [$Rh(NH_3)_4(H_2O)OOH^{2+}$] = 2.8 x 10^{-5}–4.4 x 10^{-4} M; [$L^1Rh(H_2O)OOH^{2+}$] = 1.0 x 10^{-5}–3.2 x 10^{-5} M; [$HClO_4$] = 0.02 M = μ.

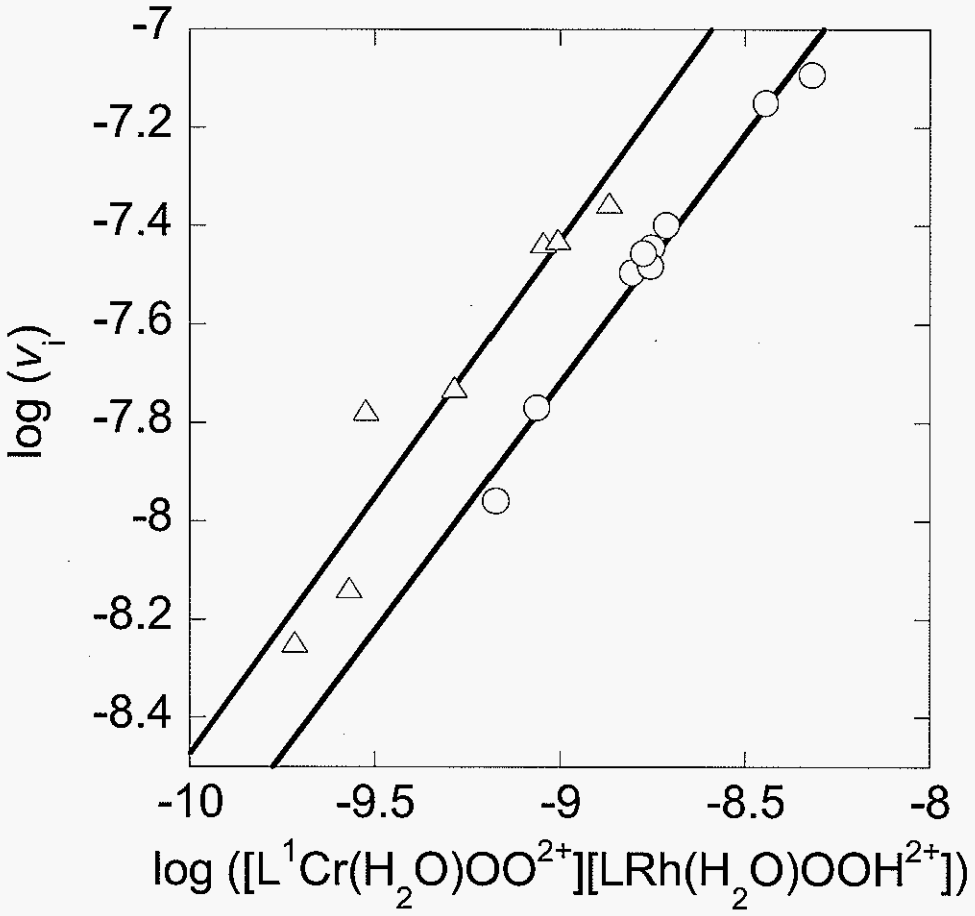

Figure 6. Log Initial rate as a function of the log ([$L^1Cr(H_2O)OO^{2+}$] x [$LRh(H_2O)OOH^{2+}$]). Slope = 1 ± .08.

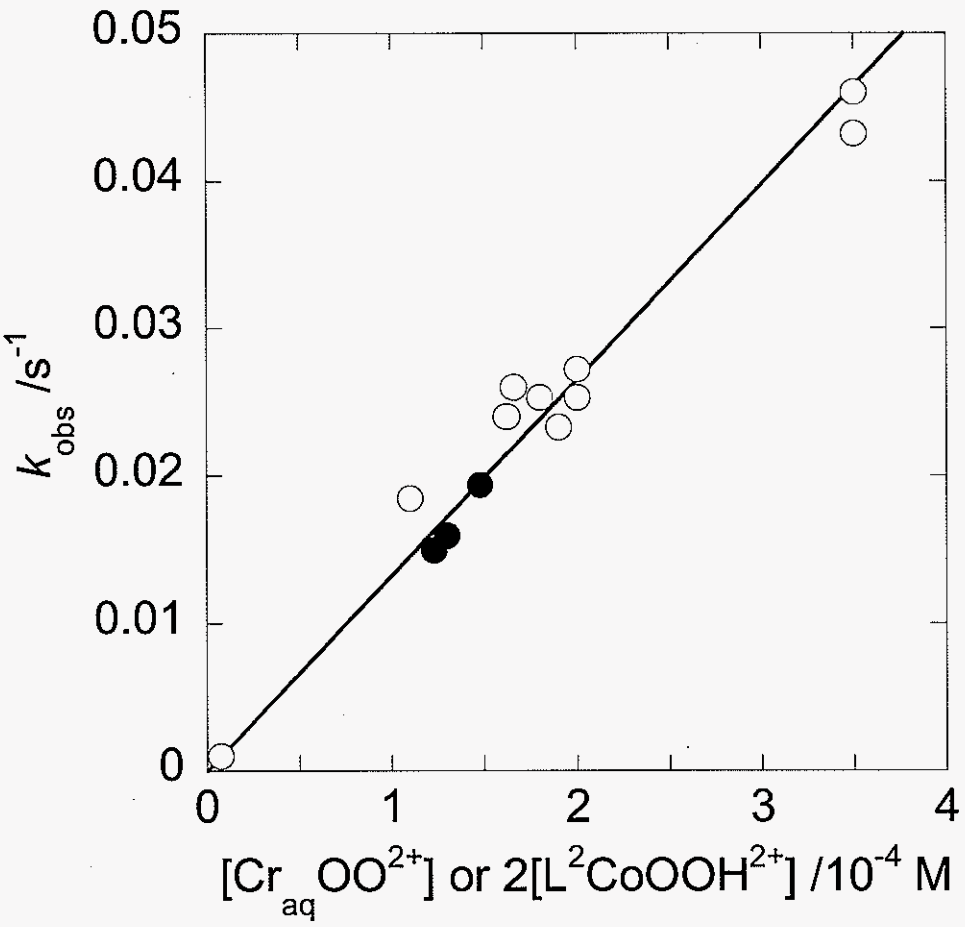

Figure 7. k_{obs} as a function of the average excess reagent concentration for the oxidation of $L^2Co(H_2O)OOH^{2+}$ with $Cr_{aq}OO^{2+}$ at 25 °C. ● = $[Cr_{aq}OO^{2+}]_{avg}$, ○ = $2[L^2Co(H_2O)OOH^{2+}]_{avg}$. Slope = k = 130 ± 20 M^{-1} s^{-1}. Conditions: $[Cr_{aq}OO^{2+}]$ = 3 x 10^{-5}–1.5 x 10^{-4} M; $[L^2Co(H_2O)OOH^{2+}]$ = 3.2 x 10^{-5}–2.3 x 10^{-4} M; $[HClO_4]$ = 0.05 M = μ.

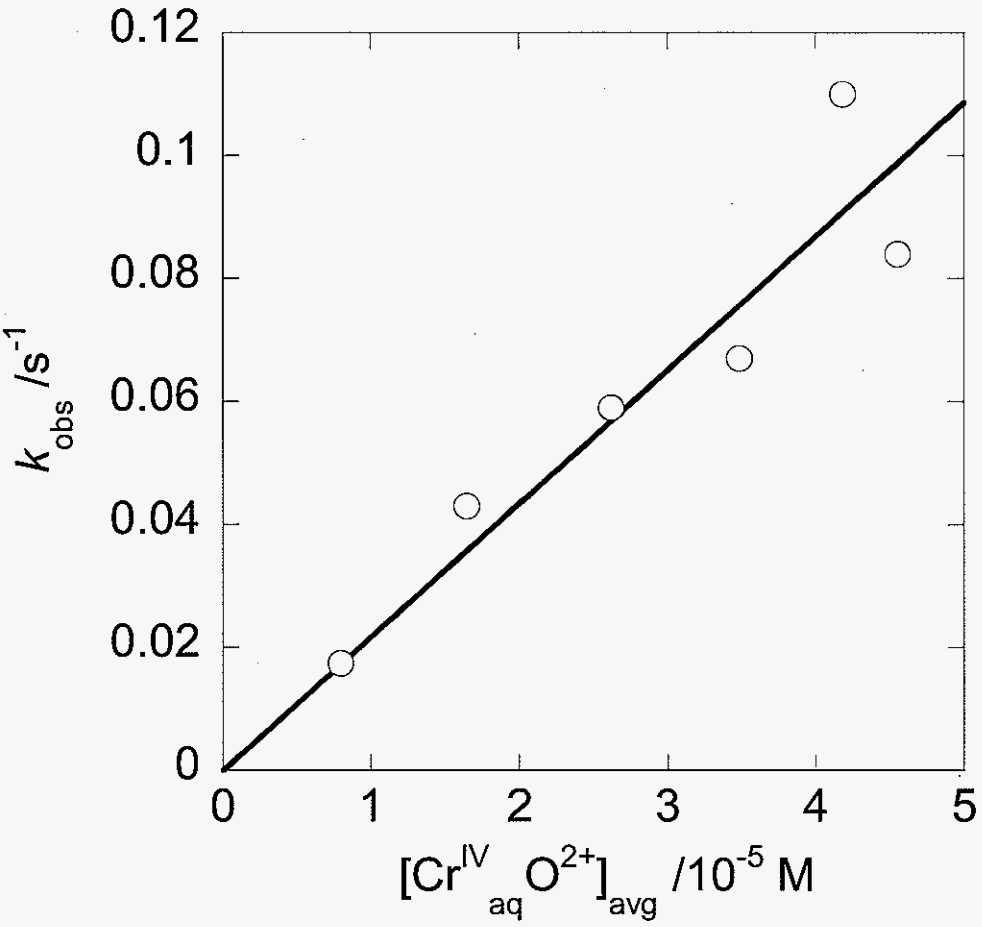

Figure 8. k_{obs} as a function of the average $[Cr^{IV}(D_2O)_5O^{2+}]$ for the reaction with $Rh(NH_3)_4(D_2O)OOD^{2+}$ at 25 °C. Slope = $k = 2 \pm 0.2 \times 10^3$ M^{-1} s^{-1}. Conditions: $[Rh(NH_3)_4(D_2O)OOD^{2+}] = 5 \times 10^{-6}$–$1 \times 10^{-5}$ M; $[DClO_4] = 0.1$ M = μ ; D/H > 98% D.

References

(1) Weinstein, J.; Bielski, B. H. J. *J. Am. Chem. Soc.* **1979**, *101*, 58-62.

(2) Chavez, F. A.; Mascharak, P. K. *Acc. Chem. Res.* **2000**, *33*, 539-545.

(3) Parshall, G. W.; Ittel, S. D. *Homogeneous Catalysis*; 2nd Ed. ed.; Wiley-Interscience: New York, 1992.

(4) Que, L., Jr. *J. Biol. Inorg. Chem.* **2004**, *9*, 684-690.

(5) Burger, R. M. *Chem. Rev.* **1998**, *98*, 1153-1169.

(6) Wolkenberg, S. E.; Boger, D. L. *Chem. Rev.* **2002**, *102*, 2477-2495.

(7) Kang, C.; Anson, F. C. *Inorg. Chem.* **1994**, *33*, 2624-2630.

(8) Bakac, A.; Espenson, J. H. *Inorg. Chem.* **1992**, *31*, 1108-1110.

(9) Bakac, A.; Thomas, L. M. *Inorg. Chem.* **1996**, *35*, 5880-5884.

(10) Bakac, A.; Espenson, J. H. *J. Am. Chem. Soc.* **1990**, *112*, 2273-2278.

(11) Bakac, A.; Wang, W. D. *Inorg. Chim. Acta* **2000**, *297*, 27-35.

(12) Pestovsky, O.; Bakac, A. *Inorg. Chem.* **2002**, *41*, 3975-3982.

(13) Wang, W.-D.; Bakac, A.; Espenson, J. H. *Inorg. Chem.* **1995**, *34*, 4049-4056.

(14) Kumar, K.; Endicott, J. F. *Inorg. Chem.* **1984**, *23*, 2447-2452.

(15) Scott, S. L.; Bakac, A.; Espenson, J. H. *J. Am. Chem. Soc.* **1991**, *113*, 7787-7788.

(16) Wang, W. D.; Bakac, A.; Espenson, J. H. *Inorg. Chem.* **1993**, *32*, 5034-5039.

(17) Bakac, A. *J. Am. Chem. Soc.* **2002**, *124*, 9136-9144.

(18) Hyde, M. R.; Espenson, J. H. *J. Am. Chem. Soc.* **1976**, *98*, 4463-4469.

(19) Dunford, H. B. *Coord. Chem. Rev.* **2002**, *233-234*, 311-318.

(20) Zhang, M.; van Eldik, R.; Espenson, J. H.; Bakac, A. *Inorg. Chem.* **1994**, *33*, 130-133.

(21) Marchaj, A.; Bakac, A.; Espenson, J. H. *Inorg. Chem.* **1992**, *31*, 4164-4168.

(22) Roth, J. P.; Yoder, J. C.; Won, T.-J.; Mayer, J. M. *Science* **2001**, *294*, 2524-2526.

(23) Mayer, J. M. *Annu. Rev. Phys. Chem.* **2004**, *55*, 363-390.

(24) Mayer, J. M. *Acc. Chem. Res.* **1998**, *31*, 441-450.

(25) Pearson, R. G. *Chem. Rev.* **1985**, *85*, 41-49.

(26) Luo, Y.-R. *Handbook of Bond Dissociation Energies in Organic Compounds*; CRC Press: Boca Raton, 2003.

(27) Bakac, A. *J. Am. Chem. Soc.* **1997**, *119*, 10726-10731.

(28) Nemes, A.; Bakac, A. *Inorg. Chem.* **2001**, *40*, 746-749.

(29) Al-Ajlouni, A.; Bakac, A.; Espenson, J. H. *Inorg. Chem.* **1993**, *32*, 5792-5796.

(30) Bakac, A.; Guzei, I. A. *Inorg. Chem.* **2000**, *39*, 736-740.

(31) Al-Ajlouni, A. M.; Espenson, J. H.; Bakac, A. *Inorg. Chem.* **199** *32*, 3162-3165.

CHAPTER II. REACTIONS OF NITROXYL RADICALS WITH SUPEROXOMETAL COMPLEXES OF CHROMIUM AND RHODIUM.

Michael J. Vasbinder and Andreja Bakac.

A manuscript submitted to *Inorganic Chemistry*.

Abstract

The persistent nitroxyl radicals of the 4-substituted-2,2,6,6-tetramethylpiperidine-*N*-oxyl radical (TEMPO) series were oxidized by superoxometal ions of Rh and Cr. Rate constants for this reaction were determined and correlated to the redox potentials of the nitroxyl radicals according to the Marcus equation. The kinetics are largely acid independent for $Cr_{aq}OO^{2+}$, but acid-catalysis dominates the reactions of the rhodium complex. The rate constants are several orders of magnitude lower than those for other common inorganic radicals reacting with nitroxyl radicals.

Introduction

Persistent nitroxyl radicals, $R_2NO\bullet$, have been known for over 40 years.[1] Their practical uses, along with their hydroxylamine and oxoammonium derivatives (Chart 1.), include gentle initiators in free-radical polymerizations[2], efficient catalysts in the selective two-electron oxidation of alcohols to ketones,[3-5] as electrocatalysts in the previous reaction[6], as well as reagents in organic synthesis.[7] They have also been extensively used as radical traps, where a reaction with the nitroxyl radical or lack there of, is used to support or disprove a radical intermediate in a reaction mechanism. Some recent uses in a diverse set of circumstances are shown in these references.[8-14]

Chart 1.

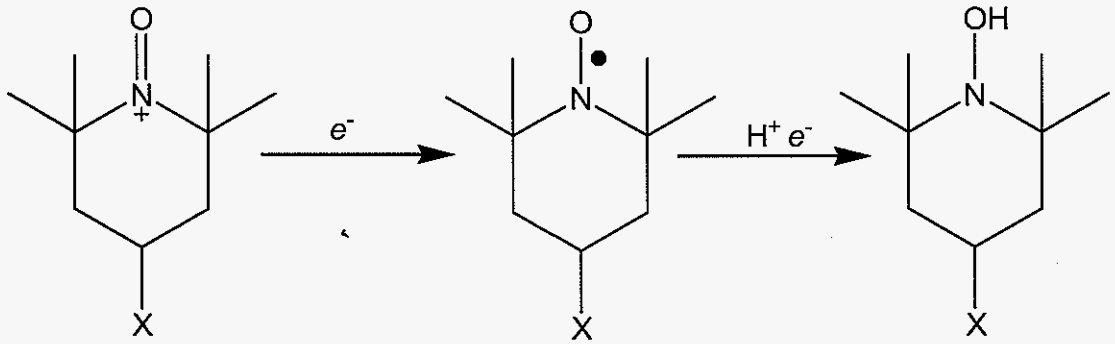

oxoammonium ion nitroxyl radical hydroxylamine

The nitroxyl radicals are of great biological interest as a spin-label[15,16] and in imaging epr[17], but more to the point in this study, because they are important antioxidants. They are particularly effective against acute physiological damage caused by reactive oxygen species.[18,19] This damage is mitigated regardless of the source of the reactive oxygen species, as both species derived from ionizing radiation[20,21] and from mechanical sources such as head trauma[22] are removed. The nitroxyl radical 2,2,6,6-tetramethylpiperidine-*N*-oxyl radical, TEMPO, efficiently

mimics the enzyme superoxide dismutase, removing toxic superoxide (O_2^-) from biological systems.[23-26]

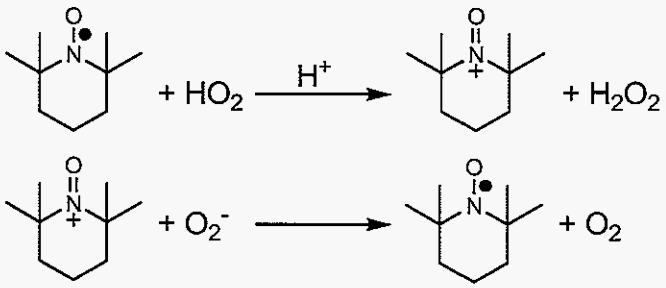

(1)

(2)

Superoxometal ions, as radical species, should react quickly a cleanly with other free radicals in solution. When $Cr_{aq}OO^{2+}$ and $Rh(NH_3)_4(H_2O)OO^{2+}$ solutions are mixed with 4-substituted 2,2,6,6-tetramethylpiperidine-*N*-oxyl radicals ((X)TEMPO), just such a reaction occurs. $Cr_{aq}OO^{2+}$ and $Rh(NH_3)_4(H_2O)OO^{2+}$ oxidize (X)TEMPO to the corresponding oxoammonium ion, the superoxide ion itself being reduced to the corresponding hydroperoxo complex.

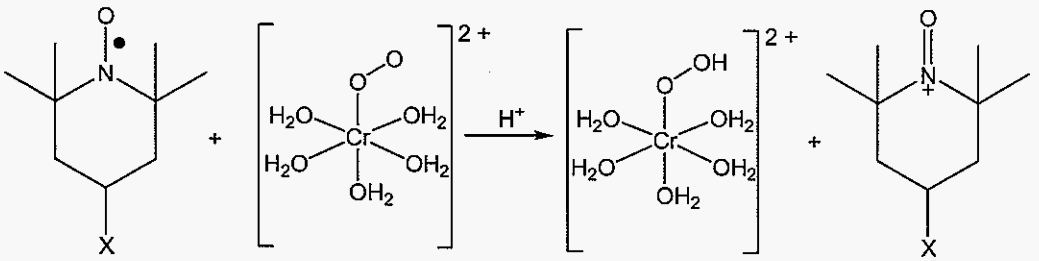

(3)

This is supported by the respective redox potentials, which are known independently and indicate the reaction should be exorgonic as written, by $K > 1 \times 10^4$ (for TEMPO and $Cr_{aq}OO^{2+}$).

Experimental

2,2,6,6-tetramethylpiperidine-*N*-oxyl radical (TEMPO), 4-OH-2,2,6,6-tetramethyl-piperidine-*N*-oxyl radical (TEMPOL or (HO)TEMPO), 4-O-2,2,6,6-tetramethyl-piperidine-*N*-oxyl radical (TEMPONE or (O)TEMPO) were purchased from Aldrich and used without further purification. $Cr_{aq}OO^{2+}$ was prepared as described in CHAPTER I of this thesis. $Rh(NH_3)_4(H_2O)OO^{2+}$ was typically prepared by the oxidation of its hydroperoxo-congener, $Rh(NH_3)_4(H_2O)OOH^{2+}$, with O_3. Excess O_3 was used to guarantee all hydroperoxide was converted to the superoxide, followed by removal of the excess O_3 by O_2 sparge. The oxoammonium chloride salts of TEMPONE and TEMPO was prepare by oxidizing the nitroxyl with Cl_2, following a literature procedure.[27,28]

Kinetic measurements were carried out by conventional UV-vis spectrophotometry using a Shimadzu 3101 PC spectrophotometer, thermostated at 25 ± 0.2 °C. The progress of the reactions were follow ed by watching the disappearance of $Cr_{aq}OO^{2+}$at 293 nm and $Rh(NH_3)_4(H_2O)OO^{2+}$ at 270 nm. Stopped-flow measurements were carried out using a thermostated OLIS RSM-1000 rapid-scanning stopped-flow spectrophotometer.

Results

Reactions of superoxometal ions with a large excess of piperidineoxyl radical followed first-order kinetics. The plots of the observed first-order rate constant $k_{obs.}$ vs. [(X)TEMPO] where X = 4-OH, O and H, with $Cr_{aq}OO^{2+}$ and $Rh(NH_3)_4(H_2O)OO^{2+}$ are linear with a slope equal to the second order rate constant, and are shown in Figures 1-3. The amplitudes of the Abs.-Time curves are consistent with the complete reduction of superoxometal ion to the hydroperoxide. In all but one case, the kinetics were independent of acid concentration and ionic strength in the range 0.02 – 0.10 M. Stopped-flow repetitive scan experiments, carried out with >1 mM (X)TEMPO, show no rapid step prior to what is observed on the conventional mixing timescale. Also, no absorbance around 350 - 400 nm, characteristic of the oxoammonium ion, could be observed in the reaction mixture even on this fast timescale. This absence of the oxoammonium ion spectrum is consistent with the relatively rapid decomposition as reported by Goldstein et al [25,26] for the TEMPOL and TEMPONE oxoammonium ions.

Experiments using excess superoxometal ion gave rate constants in good agreement with what was seen with excess piperidineoxyl radical. There was no change in the rate constant of the reaction when using excess superoxometal ion, which is consistent with 1 $Cr_{aq}OO^{2+}$:1 TEMPO-X stoichiometry, as already deduced from the amplitude of the absorbance changes. No reaction was observed between the decomposition products of the authentic oxoammonium chloride salt of TEMPONE and $Cr_{aq}OO^{2+}$. The hydroperoxides $Cr_{aq}OOH^{2+}$ and $Rh(NH_3)_4(H_2O)OOH^{2+}$ did not react with piperidineoxyl radicals.

The piperidineoxyl radicals tested did not have the ability to catalytically react with superoxometal ion, as depicted in Scheme 1. This was demonstrated in the reaction of $Cr_{aq}OO^{2+}$ with TEMPO and TEMPOL in the presence of excess methanol,

which is known to reduce the oxoammonium ions to the corresponding hydroxylamines via a $2e^-$ hydride-transfer mechanism.

$$R_2N^+{=}O + RCH_2OH \rightarrow R_2NO\text{-}H + RCHO + H^+ \qquad (4)$$

The reported rate constant for this reaction is 0.48 ± 0.02 M^{-1} s^{-1} ($TEMPO^+$, pH 6.9).[25] Typical MeOH concentrations in $Cr_{aq}OO^{2+}$ preparations were 0.1 – 0.2 M. No difference in the rate constant or stoichiometry was observed when concentrations as high as 4.7 M MeOH were used. Since there was enough methanol to efficiently trap the oxoammonium ion, the slow reaction between the hydroxylamine TEMPO-H and $Cr_{aq}OO^{2+}$ must be the cause of the lack of catalysis. We have shown independently that the hydroxylamine Et_2NO-H reacted more slowly than the corresponding nitroxyl radical with $Cr_{aq}OO^{2+}$.

Scheme 1.

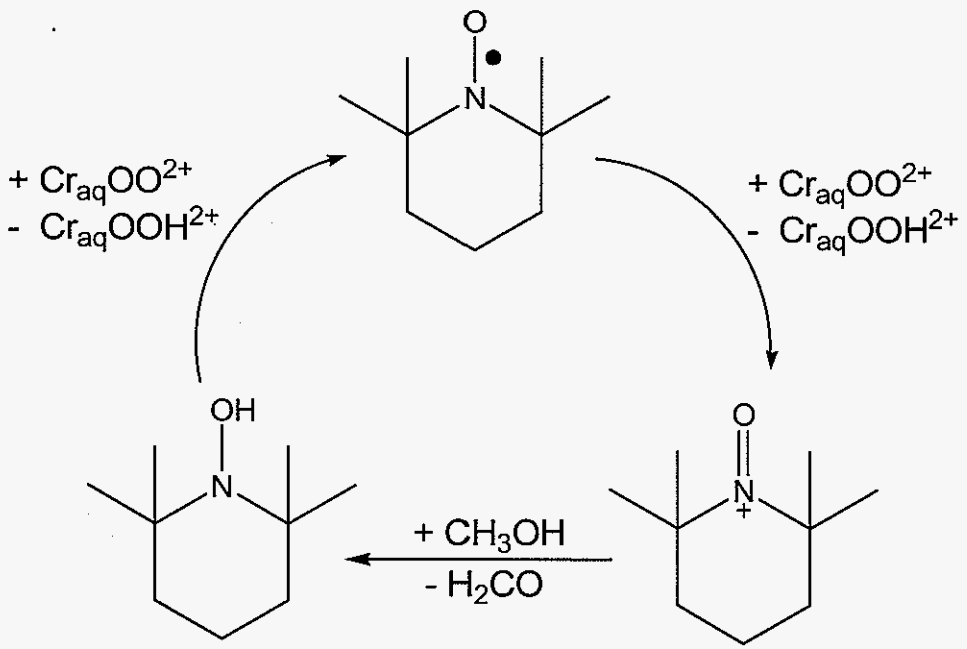

Effect of acid concentration on the observed rate constant

In the reactions of $Rh(NH_3)_4(H_2O)OO^{2+}$ with all nitroxyls, an acid-catalyzed pathway was observed. For TEMPONE oxidation, this is shown in Fig. 4 and 5, where observed second-order rate constants increase with acid concentration at a constant ionic strength. The slope of the plot of k_{obs} vs. $[H^+]$ yields a 3rd-order rate constant of $2.2 \pm 0.2 \times 10^3\ M^{-2}\ s^{-1}$. A lower limit of $<5\ M^{-1}\ s^{-1}$ could be assigned to the acid-independent path, meaning the major pathway in the reaction is acid-catalyzed. In accordance with specific acid catalysis, an inverse kinetic isotope effect of *k*H/*k*D ~0.8 was observed. as shown in Fig. 6.[29] In acidified D_2O the concentration of protonated amminerhodium superoxide, $(Rh(NH_3)_4(D_2O)OO(D)^{3+}$ vs. $Rh(NH_3)_4(H_2O)OO(H)^{3+})$ is raised, meaning more of the reactive form of the oxidant is available. This is due to the lower basicity of D_2O (D_3O^+ is a stronger acid than H_3O^+) and increased stability of $Rh(NH_3)_4(D_2O)OO(D)^{3+}$. Typical values for inverse kies in acid-catalyzed hydrolysis reactions range from *k*H/*k*D = 0.3–0.8. The acid-catalyzed oxidation of I^- with $Cr_{aq}OO^{2+}$ exhibits an inverse kinetic isotope effect of *k*H/*k*D = 0.5.[30]

The reaction of $Cr_{aq}OO^{2+}$ with TEMPONE also began to show an acid-catalyzed path, but to a much smaller extent than with $Rh(NH_3)_4(H_2O)OO^{2+}/(H)^{3+}$ as the oxidant. The plot of k_{obs} vs. [TEMPONE] in 0.02 M and 0.10 M $HClO_4$ revealed a small increase in observed rate constant when moving from lower to higher acid concentration, as can be seen in Fig. 3. The small value of the third-order rate constant of $\sim 60\ M^{-2}\ s^{-1}$ derived from this increase combined with the relatively large value of $21\ M^{-1}\ s^{-1}$ for the uncatalyzed reaction means the major pathway in TEMPONE oxidation by $Cr_{aq}OO^{2+}$ is not acid-catalyzed.

Similar effects of acid concentration on observed rate constant are seen in the oxidations of TEMPO and TEMPOL by $Rh(NH_3)_4(H_2O)OO^{2+}$. However, the

importance of the $[H^+]$-independent intercept term increases with improved thermodynamics, so that the stronger reductants, TEMPOL and, especially, TEMPO, exhibit measurable intercepts in their plots of k_{obs} against $[H^+]$, as shown in Fig. 7. The values of the 3rd-order rate constants for $Rh(NH_3)_4(H_2O)OO(H)^{3+}$ oxidation of (X)TEMPO are all similar and in the range of $1 - 2 \times 10^3$ M^{-2} s^{-1}. In contrast to this, the magnitudes of the $[H^+]$-independent term increase as a function of the reducing ability of the nitroxyls, from <5 M^{-1} s^{-1} in the difficult to oxidize, poorly reducing TEMPONE to ~ 50 M^{-1} s^{-1} for the best reductant, TEMPO. This is expected on the basis of Marcus' Theory, and more will be said on this in the following **Discussion.**

Discussion

The oxidations of piperidineoxyl radicals with $Cr_{aq}OO^{2+}$ and $Rh(NH_3)_4(H_2O)OO^{2+}$ are decidedly slower than with other free-radical oxidants, as can be seen in Table 1. Small, thermodynamically powerful radical oxidants, such as •OH and HO_2, react with rate constants approaching the diffusion controlled limit, > 10^8 M^{-1} s^{-1}. The superoxometal ions $Cr_{aq}OO^{2+}$ and $Rh(NH_3)_4(H_2O)OO^{2+}$ react with these same radicals with rate constants similar to those for closed-shell oxidants, such as I_2 and $C(NO_2)_4$. Similarly, the radical $•NO_2$, which has a reduction potential comparable to that of $Cr_{aq}OO^{2+}$, reacts with nitroxyl radicals much more quickly than the superoxometal ion does.

The rate constants for piperidineoxyl radical oxidation by superoxometal ions are proportional to the $E°$ for oxoammonium ion reduction, the plot of which can be seen in Fig. 8. This allows us to interpret the data following the Marcus cross-relation, $k_{12} = (k_{11}k_{22}K_{12}f_{12})^{1/2}$. The slope of log k vs. E (for oxoammonium ion reduction) is -7.5 for $Cr_{aq}OO^{2+}$, in good agreement with the theoretical value of -8.4. Marcus theory predicts slower rate constants for oxidation of piperidineoxyl radicals

as the driving force of the reaction is decreased, in this case, by increasing the value of *E* for the (X)TEMPO$^+$ / (X)TEMPO couple by substitution on the ring, meaning the poorer a reductant the nitroxyl is, the slower its oxidation should take place. Similar agreements with the Marcus equation have been obtained for the oxidation of this series of piperidineoxyl radicals by tetranitromethane[31,32], and for the oxidation of TEMPO and 3-carbamyl-PROXYL (PROXYL = 2,2,5,5-tetramethylpyrolidinoxyl radical) by hydroperoxyl radical[25]. These results are summarized in Table 1.

Marcus theory also allows for the estimation of the potential of the $Rh(NH_3)_4(H_2O)OO^{2+}$/-OOH^{2+} couple. The direct electrochemical measurement for this couple is unavailable due to complexities in the electrochemistry. It is fair to assume similar self-exchange rate constants for superoxometal ions, since each are substitutionaly inert complexes with small ligands. A comparison of the rate of reaction between metal superoxide and nitroxyl, as well as the known potentials for the $Cr_{aq}OO^{2+}$/-OOH^{2+} and piperidineoxyl radical couples (see Table 1) allows for the estimation of *K* ($\Delta E°$) for the $Rh(NH_3)_4(H_2O)OO^{2+}$ + (X)TEMPO reaction. From this $\Delta E°$, the $E°$ for $Rh(NH_3)_4(H_2O)OO^{2+}$/-OOH^{2+} can be calculated by comparing back to known piperidineoxyl radical potentials. This exercise places $Rh(NH_3)_4(H_2O)OO^{2+}$/-OOH^{2+} in the range of 0.93–1 V. The calculation is shown in the **Supplemental**. Support for using Marcus theory to estimate the value of the rhodium couple comes from the increasing value of the [H^+]-independent term as a function of (X)TEMPO potentials.

This $E°$ derived from the Marcus correlation is likely larger than the real value, as deduced from studying eq 6 in Chapter I of this thesis.

$$Cr_{aq}OO^{2+} + Rh(NH_3)_4(H_2O)OOH^{2+} = Cr_{aq}OOH^{2+} + Rh(NH_3)_4(H_2O)OO^{2+} \quad K_6 \quad (6)$$

Since no reverse reaction is observed between $Rh(NH_3)_4(H_2O)OO^{2+}$ and $Cr_{aq}OOH^{2+}$, the limiting value of K_6 can be placed at $\geq$46, corresponding to an E° for the $Rh(NH_3)_4(H_2O)OO^{2+}/\text{-}OOH^{2+}$ couple at $\leq$0.93 V. As can be seen in Fig. 6 and Table 1., all reactions using $Rh(NH_3)_4(H_2O)OO^{2+}$ as oxidant are slower relative to $Cr_{aq}OO^{2+}$, suggesting $Cr_{aq}OO^{2+}$ is the more powerful oxidant. This is consistent with what is known for the reaction in eq 6. A value for the $Rh(NH_3)_4(H_2O)OO^{2+}/\text{-}OOH^{2+}$ E° in this range would also mean a small driving force for the reaction of $Rh(NH_3)_4(H_2O)OO^{2+}$ with (X)TEMPO, requiring acid-catalysis to drive the reactions by protonating the oxidant, as is seen in this case, and to a lesser extent for $Cr_{aq}OO^{2+}$ with TEMPONE.

Conclusion

Superoxometal ions of Cr and Rh do indeed oxidize the piperidineoxyl radicals of the (X)TEMPO series. The rate constants are many orders of magnitude smaller than those observed for other common inorganic radicals with these same nitroxyl radicals. The rate constants for the reaction of superoxometal ions with (X)TEMPO are more in line with those of closed shell oxidants, the kinetic barrier reflecting the highly delocalized nature of these superoxometal ions. In the most downhill reactions, those involving $Cr_{aq}OO^{2+}$ with TEMPO and TEMPOL, no effect of acid concentration or ionic strength is observed on the rate constant. However, in reactions with a smaller thermodynamic driving force, acid-catalysis is necessary for the reaction to proceed at an appreciable rate. The rate constants correlate with the known redox potentials of the oxoammonium ion/nitroxyl radical couples and the $Cr_{aq}OO^{2+}/\text{-}OOH^{2+}$ couple. These results fit the Marcus' cross-relation for electron transfer, showing agreement within 15% of the theoretical value.

Table 1. Comparison of electron-transfer reactions of piperidineoxyl radicals with various oxidants.

oxidant	nitroxyl	k (M^{-1} s^{-1})	$E°$ox.[a]	$E°_{R_2NO^+}$[b]	Ref.
$Cr_{aq}OO^{2+}$	TEMPO	406 ± 12	1.03	0.73	*c*
$Cr_{aq}OO^{2+}$	TEMPOL	159 ± 3	1.03	0.80	*c*
$Cr_{aq}OO^{2+}$	TEMPONE	21 ± 1	1.03	0.91	*c*
$Rh(NH_3)_4(H_2O)OO^{2+}$	TEMPO	50 ± 15 [d]	≤0.93	0.73	*c*
$Rh(NH_3)_4(H_2O)OO^{2+}$	TEMPOL	25 ± 5 [d]	≤0.93	0.80	*c*
$Rh(NH_3)_4(H_2O)OO^{2+}$	TEMPONE	<5 [d]	≤0.93	0.91	*c*
I_2	TEMPO	5.3	0.21[e]	0.73	*33*
$C(NO_2)_4$	TEMPO	6.6	0.93	0.73	*34*
$C(NO_2)_4$	TEMPOL	0.85	0.93	0.80	*34*
$C(NO_2)_4$	TEMPONE	0.075	0.93	0.91	*32*
HO_2	TEMPO	$1.2 \pm 0.1 \times 10^8$	1.44	0.73	*25*
$O_2^{\bullet-}$	TEMPO	$<1 \times 10^3$	0.88	0.73	*25*
HO_2	3-CP[f]	$1.3 \pm 0.1 \times 10^6$	1.44	0.87	*25*
•OH	TEMPO	$4.5 \pm 0.4 \times 10^9$	2.72	0.73	*35*
•OH	TEMPOL	$4.5 \pm 0.4 \times 10^9$	2.72	0.80	*35*
•OH	TEMPONE	$4.5 \pm 0.4 \times 10^9$	2.72	0.91	*35*
•OH	3-CP[f]	3.7×10^9	2.72	0.87	*36*
$•NO_2$	TEMPO	$7.1 \pm 0.2 \times 10^8$	1.04	0.73	*26*
$•NO_2$	TEMPOL	$8.7 \pm 0.2 \times 10^8$	1.04	0.80	*26*
$•NO_2$	TEMPONE	$7.1 \pm 0.2 \times 10^8$	1.04	0.91	*26*
$•NO_2$	3-CP[f]	$7.1 \pm 0.2 \times 10^8$	1.04	0.87	*26*
$Ru(bpy)_3^{3+}$	3-CP[f]	$4.9 \pm 0.2 \times 10^8$	1.29	0.87	*37*

a Volts vs. NHE, $X + e^- + H^+ \rightarrow XH$. Ref. [38,39]

b $R_2N^+=O/ R_2NO$, Volts vs. NHE Ref.[40-42]

c This work.

d Represents the extrapolated zero acid constant as derived from the intercept of the plots of *k* vs acid concentration (Figs. 5 and 7). 3rd-order rate constants are:

$2.2 \pm 0.2 \times 10^3\ M^{-2}\ s^{-1}$ for TEMPONE

$1.1 \pm 0.2 \times 10^3\ M^{-2}\ s^{-1}$ for TEMPOL

$2.2 \pm 0.2 \times 10^3\ M^{-2}\ s^{-1}$ for TEMPO

e For $I_2 + e^- \rightarrow I_2^-$ initial step. Net reaction $I_2 + 2R_2NO \rightarrow 2I^- + 2R_2N^+=O$

f 3-CP = 3-carbamyl-PROXYL radical

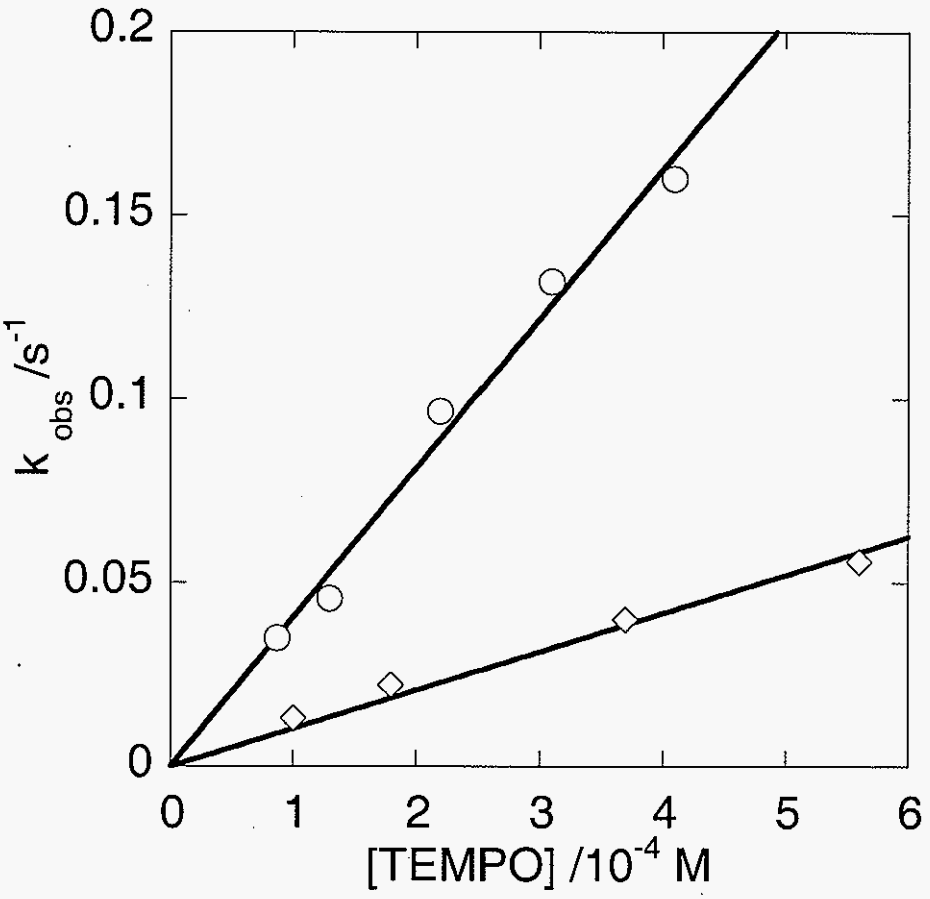

Figure 1. The plot of k_{obs} vs. [TEMPO] concentration for the reaction of superoxometal ions with TEMPO at 25 °C. Condition s: ○ $[Cr_{aq}OO^{2+}]$ = 1.3-7.0 x 10^{-5} M; Slope = k = 406 ± 12 M^{-1} s^{-1};

◇ $[Rh(NH_3)_4(H_2O)OO^{2+}]$ = 1-1.2 x 10^{-5} M; Slope = 104 ± 4 M^{-1} s^{-1};

$[HClO_4]$ = 0.02 – 0.10 M. μ = 0.02 – 0.12 M ($NaClO_4$ balance).

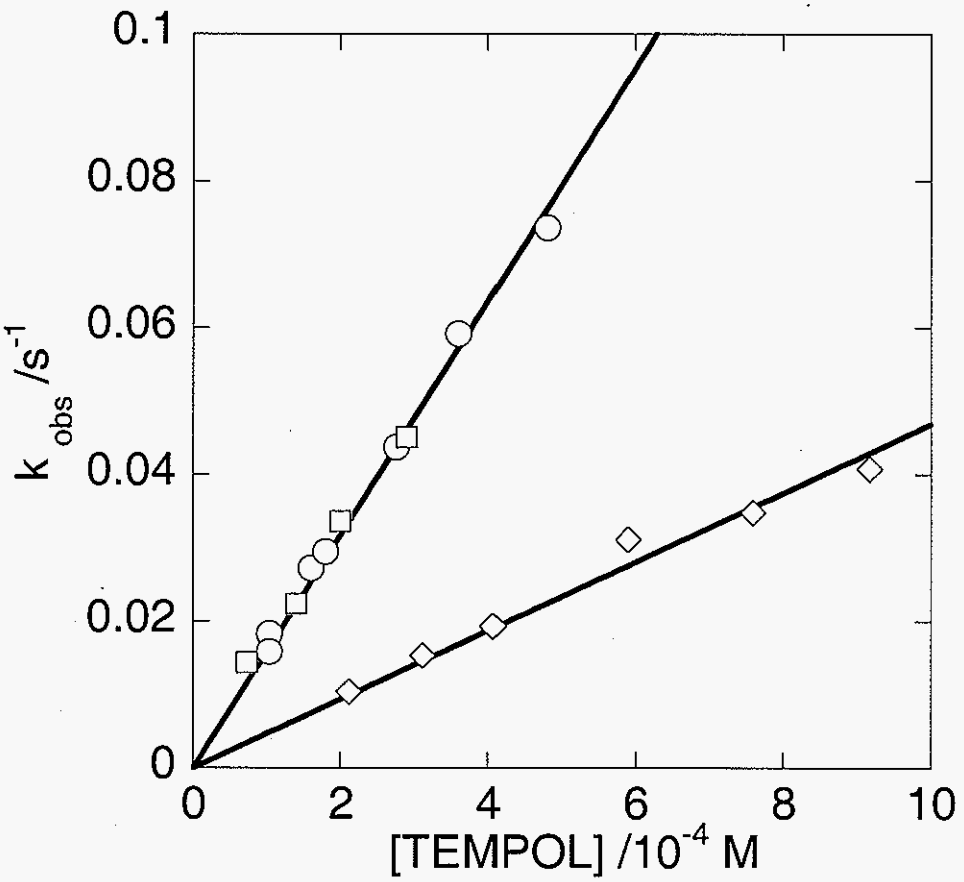

Figure 2. k_{obs} vs. [TEMPOL] concentration for the reaction of superoxometal ions with TEMPOL at 25 °C. Conditions: ○,□ [$Cr_{aq}OO^{2+}$] = 0.8-3.2 x 10^{-5} M; ○ in 0.02 M $HClO_4$; □ in 0.10 M $HClO_4$;

◇ [$Rh(NH_3)_4(H_2O)OO^{2+}$] = 0.8- 3.2 x 10^{-5} M; Slope = k = 159 ± 3 M^{-1} s^{-1} for $Cr_{aq}OO^{2+}$ and 47 ± 3 M^{-1} s^{-1} for $Rh(NH_3)_4(H_2O)OO^{2+}$.

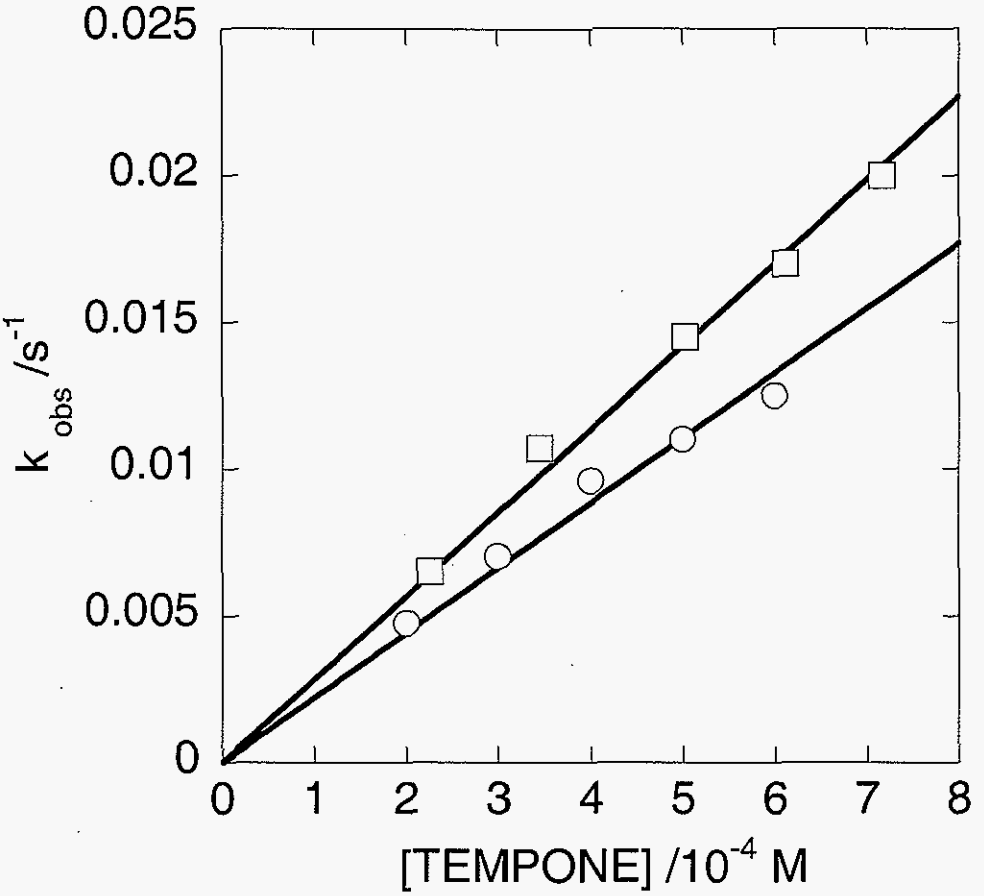

Figure 3. k_{obs} vs. [TEMPONE] concentration for the reaction of $Cr_{aq}OO^{2+}$ with TEMPONE at 25 °C. Conditions: ○ in 0.02 M $HClO_4$; □ in 0.10 M $HClO_4$; $[Cr_{aq}OO^{2+}] = 3.4 - 9.0 \times 10^{-5}$ M; Slope = $k = 28 \pm 0.5$ M^{-1} s^{-1} for □; 22 ± 0.6 M^{-1} s^{-1} for ○; $\mu = 0.1$ M ($NaClO_4$ balance).

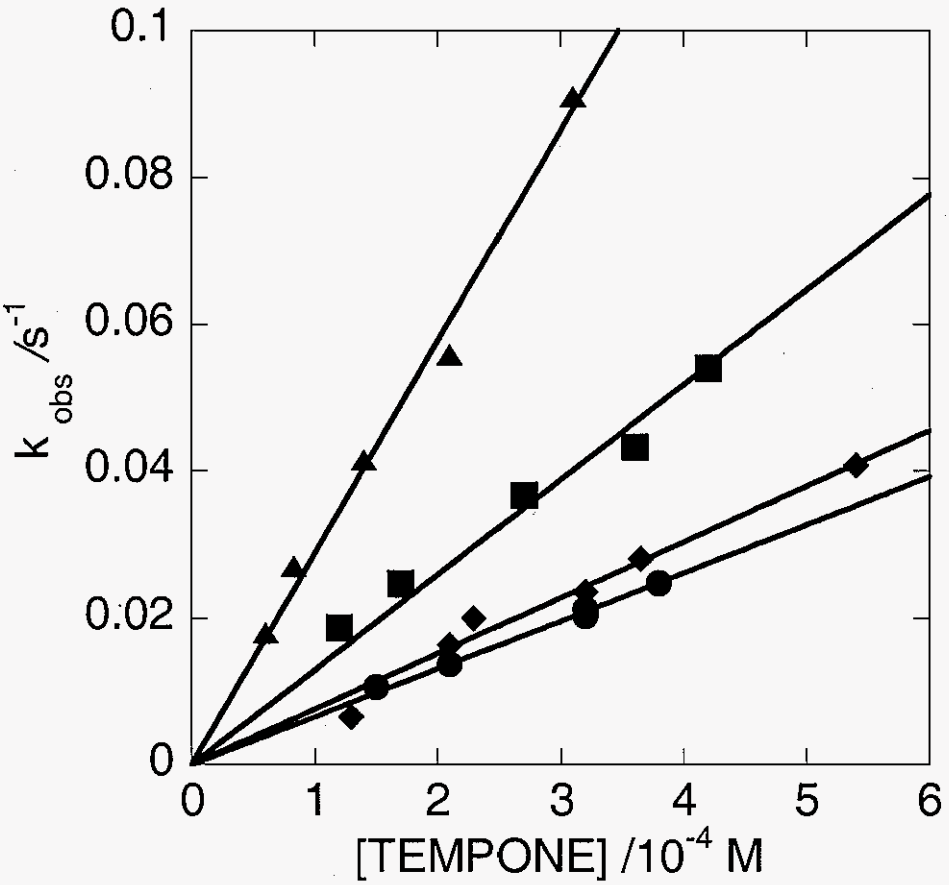

Figure 4. k_{obs} vs. [TEMPONE] concentration for the reaction of $Rh(NH_3)_4(H_2O)OO^{2+}$ with TEMPONE at 25 °C in indicated [$HClO_4$]. Conditions: = [$Rh(NH_3)_4(H_2O)OO^{2+}$] = 0.3 - 3.0 x 10^{-5} M; ● = 0.02 M $HClO_4$, slope = 65 ± 1 M^{-1} s^{-1}; ◆ = 0.04 M $HClO_4$, slope = 78 ± 2 M^{-1} s^{-1}; ■ = 0.066 M $HClO_4$, slope = 129 ± 4 M^{-1} s^{-1}; ▲ = 0.10 M $HClO_4$, slope = 237 ± 8 M^{-1} s^{-1}; μ = 0.1 M ($NaClO_4$ balance).

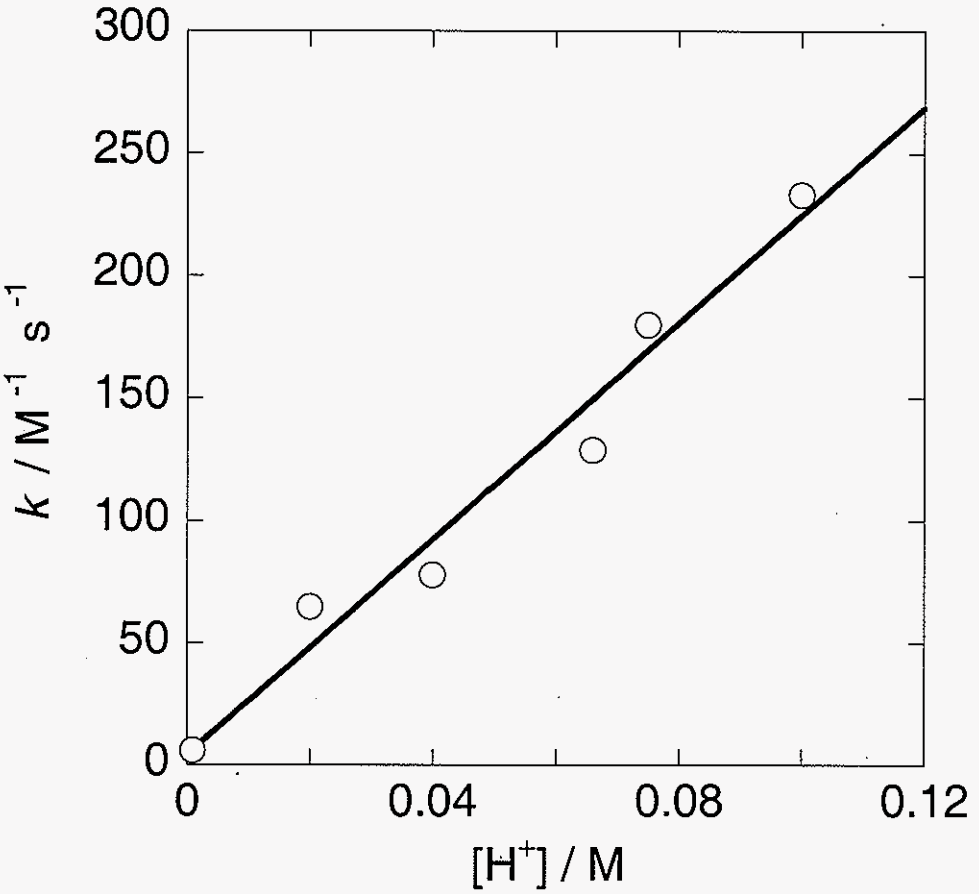

Figure 5. Apparent second-order rate constant for $Rh(NH_3)_4(H_2O)OO^{2+}$ + TEMPONE vs. acid concentration at 25 °C. Slope = $k = 2.2 \pm 0.2 \times 10^3\ M^{-2}\ s^{-1}$; $\mu = 0.1$ M ($NaClO_4$ balance).

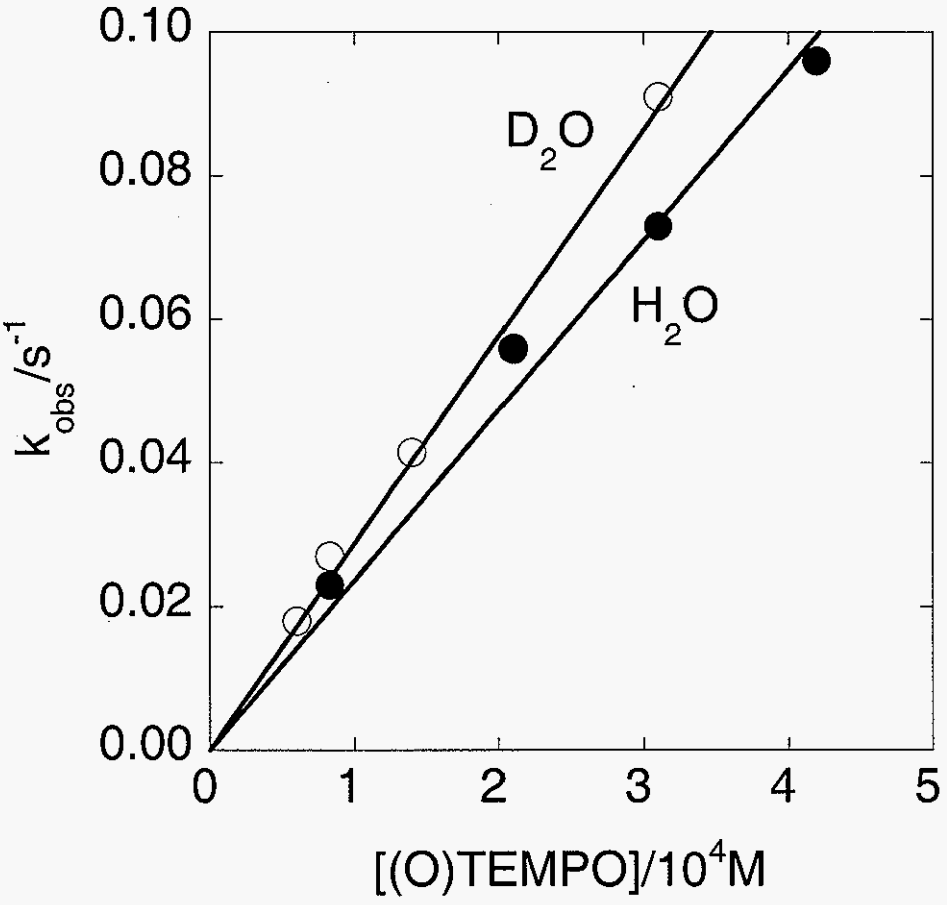

Figure 6. Change in observed rate constant for the reaction of TEMPONE with $(NH_3)_4(H(D))_2O)RhOO^{2+}$ in 0.10 M $H(D)ClO_4$ in H_2O and D_2O at 25 °C. In D_2O, slope = k = 288 ± 8 M^{-1} s^{-1}. For H_2O, 237 ± 8 M^{-1} s^{-1}.

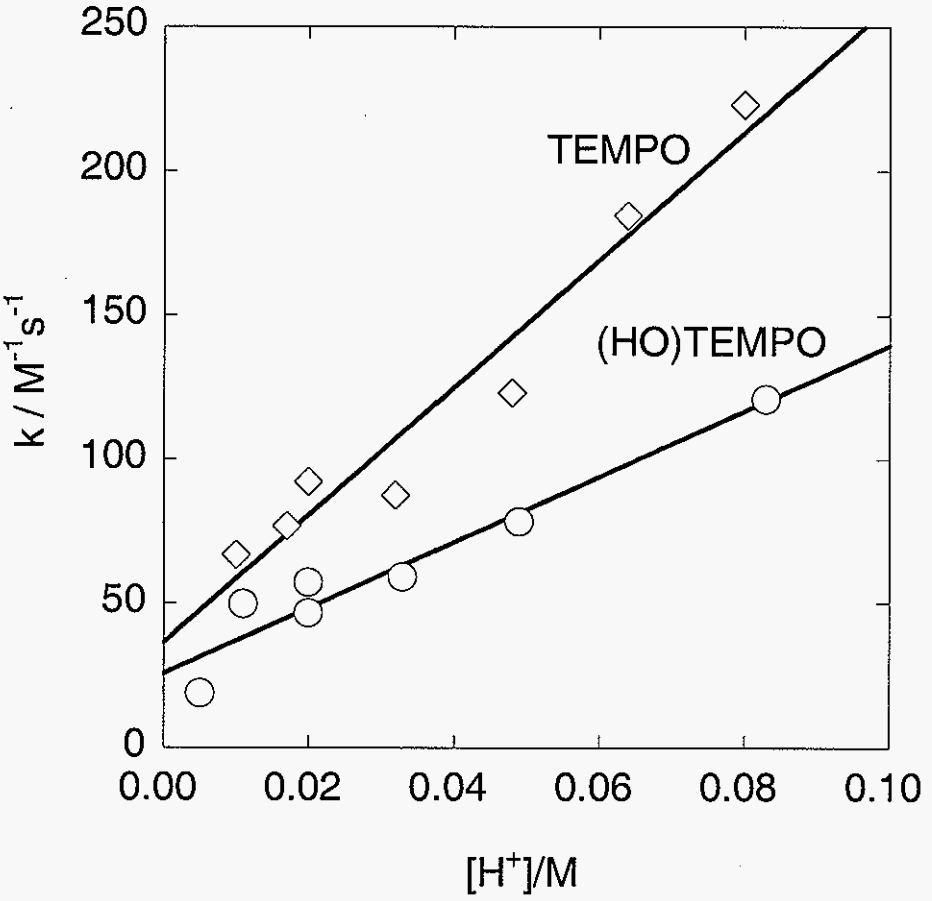

Figure 7. Apparent second-order rate constant for the reaction of $Rh(NH_3)_4(H_2O)OO^{2+}$ with TEMPO and TEMPOL ((HO)TEMPO) vs. acid concentration at 25 °C. Slope = $k = 2.2 \pm 0.2 \times 10^3\ M^{-2}\ s^{-1}$, intercept = $50 \pm 15\ M^{-1}\ s^{-1}$ for TEMPO. Slope = $k = 1.1 \pm 0.2 \times 10^3\ M^{-2}\ s^{-1}$, intercept = $25 \pm 5\ M^{-1}\ s^{-1}$ for TEMPOL. μ = 0.1 M ($NaClO_4$ balance).

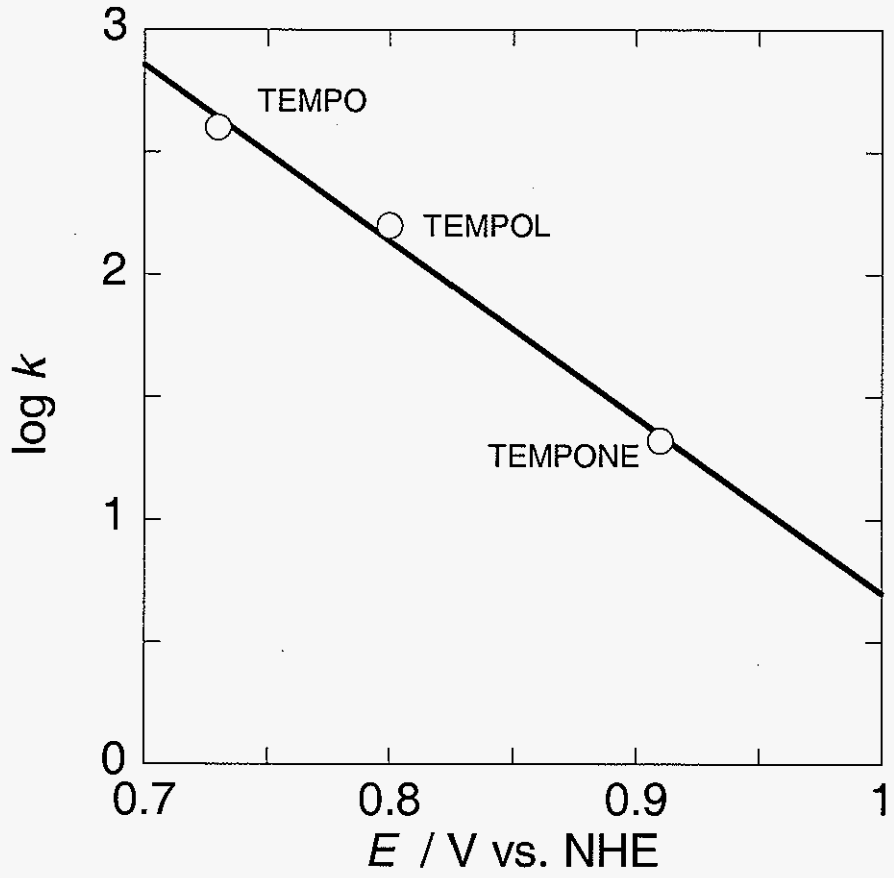

Figure 8. log k vs the reduction potential (vs. NHE) of (X)TEMPO$^+$/(X)TEMPO for the reaction with $Cr_{aq}OO^{2+}$

References

(1) Rozantsev, E. G. *Free Nitroxyl Radicals*; Plenum: New York, 1970.

(2) Nilsen, A.; Braslau, R. *J. Polym. Sci., Part A: Polym. Chem.* **2005**, *44*, 697-717.

(3) Sheldon, R. A.; Arends, I. W. C. E. *Adv. Synth. Catal.* **2004**, *346*, 1051-1071.

(4) Sheldon, R. A.; Arends, I. W. C. E.; ten Brink, G.-J.; Dijksman, A. *Acc. Chem. Res.* **2002**, *35*, 774-781.

(5) Dijksman, A.; Marino-Gonzalez, A.; Mairata i Payeras, A.; Arends, I. W. C. E.; Sheldon, R. A. *J. Am. Chem. Soc.* **2001**, *123*, 6826-6833.

(6) Semmelhack, M. F.; Chou, C. S.; Cortes, D. A. *J. Am. Chem. Soc.* **1983**, *105*, 4492-4494.

(7) Merbouh, N. *Synlett* **2003**, 1757-1758.

(8) Yin, C.-X.; Finke, R. G. *Inorg. Chem.* **2005**, *44*, 4175-4188.

(9) Wright, P. J.; English, A. M. *J. Am. Chem. Soc.* **2003**, *125*, 8655-8665.

(10) Slaughter, L. M.; Collman, J. P.; Eberspacher, T. A.; Brauman, J. I. *Inorg. Chem.* **2004**, *43*, 5198-5204.

(11) Stolzenberg, A. M.; Cao, Y. *J. Am. Chem. Soc.* **2001**, *123*, 9078-9090.

(12) Kiani, S.; Tapper, A.; Staples, R. J.; Stavropoulos, P. *J. Am. Chem. Soc.* **2000**, *122*, 7503-7517.

(13) Goodwin, J. M.; Olmstead, M. M.; Patten, T. E. *J. Am. Chem. Soc.* **2004**, *126*, 14352-14353.

(14) Albeniz, A. C.; Espinet, P.; Lopez-Fernandez, R.; Sen, A. *J. Am. Chem. Soc.* **2002**, *124*, 11278-11279.

(15) Stone, T. J.; Buckman, T.; Nordio, P. L.; McConnell, H. M. *Proc. Natl. Acad. Sci.* **1965**, *54*, 1010-1017.

(16) Keana, J. F. W. *Chem. Rev.* **1978**, *78*, 37-64.

(17) Berliner, J. L.; Fujii, H. *Science.* **1985**, *227*, 517-519.

(18) Mitchell, J. B.; Russo, A.; Kuppusamy, P.; Krishna, M. C. *Ann. N. Y. Acad. Sci.* **2000**, *899*, 28-43.

(19) Mitchell, J. B.; Krishna, M. C.; Samuni, A.; Russo, A.; Hahn, S. M. In *Reactive Oxygen Species in Biological Systems: An Interdisciplinary Approach*; Gilbert, D. L., Colton, C. A., Eds.; Plenum: New York, 1999.

(20) Mitchell, J. B.; DeGraff, W.; Kaufman, D.; Krishna, M. C.; Samuni, A.; Finkelstein, E.; Ahn, M. S.; Hahn, S. M.; Gamson, J.; Russo, A. *Arch. Biochem. Biophys.* **1991**, *289*, 62-70.

(21) Hahn, S. M.; Wilson, L.; Krishna, C. M.; Liebmann, J.; DeGraff, W.; Gamson, J.; Samuni, A.; Venzon, D.; Mitchell, J. B. *Radiat. Res.* **1992**, *132*, 87-93.

(22) Zhang, R.; Shohami, E.; Beit-Yannai, E.; Bass, R.; Trembovler, V.; Samuni, A. *Free Radic. Biol. Med.* **1998**, *24*, 332–340.

(23) Krishna, M. C.; Grahame, D. A.; Samuni, A.; Mitchell, J. B.; Russo, A. *Proc. Natl. Acad. Sci.* **1992**, *89*, 5537-5541.

(24) Krishna, M. C.; Russo, A.; Mitchell, J. B.; Goldstein, S.; Dafni, H.; Samuni, A. *J. Biol. Chem.* **1996**, *271*, 26026-26031.

(25) Goldstein, S.; Merenyi, G.; Russo, A.; Samuni, A. *J. Am. Chem. Soc.* **2003**, *125*, 789-795.

(26) Goldstein, S.; Samuni, A.; Russo, A. *J. Am. Chem. Soc.* **2003**, *125*, 8364-8370.

(27) Golubev, V. A.; Zhdanov, R. I.; Rozantsev, E. G. *Izv. Akad. Nauk. SSR, Ser. Khim.* **1970**, 184-185.

(28) Hunter, D. H.; Racok, J. S.; Rey, A. W.; Zea-Ponce, Y. *J. Org. Chem.* **1988**, *53*, 1278-1281.

(29) Wiberg, K. B. *Chem. Rev.* **1955**, *55*, 713-743.

(30) Bakac, A.; Shi, C.; Pestovsky, O. *Inorg. Chem.* **2004**, *43*, 5416-5421.

(31) Vorob'eva, T. P.; Kozlov, Y. N.; Kokorin, A. I.; Petrov, A. N. *Khim. Fiz.* **1982**, 1518-1524.

(32) Vorob'eva, T. P.; Durova, E. L.; Kozlov, Y.; Petrov, A. N.; Purmal, A. P. *Zh. Fiz. Khim.* **1986**, *60*, 598-602.

(33) Sen, V. D.; Golubev, V. A.; Kosheleva, T. M. *Izv. Akad. Nauk. SSR, Ser. Khim.* **1977**, 747-753.

(34) Petrov, A. N.; Kozlov, Y. N. *Zh. Fiz. Khim.* **1986**, *60*, 327-331.

(35) Samuni, A.; Goldstein, S.; Russo, A.; Mitchell, J. B.; Krishna, M. C.; Neta, P. *J. Am. Chem. Soc.* **2002**, *124*, 8719-8724.

(36) Asmus, K. D.; Nigam, S.; Willson, R. L. *Int. J. Radiat. Biol.* **1976**, *29*, 211-219.

(37) Ford, W. E.; Rodgers, M. A. J. *J. Phys. Chem. B* **1997**, *101*, 930-936.

(38) Kang, C.; Anson, F. C. *Inorg. Chem.* **1994**, *33*, 2624-2630.

(39) Stanbury, D. M. *Adv. Inorg. Chem.* **1989**, *33*, 69-138.

(40) Fish, J. R.; Swarts, S. G.; Sevilla, M. D.; Malinski, T. *J. Phys. Chem.* **1988**, *92*, 3745-3751.

(41) Kato, Y.; Shimizu, Y.; Yijing, L.; Unoura, K.; Utsumi, H.; Ogata, T. *Electrochim. Acta* **1995**, *40*, 2799-2802.

(42) Morris, S.; Sosnovsky, G.; Hui, B.; Huber, C. O.; Rao, N. U. M.; Swartz, H. M. *J. Pharm. Sci.* **1991**, *80*, 149-152.

Supplemental

Calculation of E° for $Rh(NH_3)_4(H_2O)OO^{2+}/\text{-}OOH^{2+}$

$k_{12} = (k_{11}k_{22}K_{12}f_{12})^{1/2}$

$f_{12} \sim 1$ (assumed)

$LMOO + LM'OOH \rightarrow LMOOH + LM'OO$ k_{11} assumed 1:1 for Cr and Rh

$R_2N^+{=}O + R_2N'O \rightarrow R_2NO + R_2N'^+{=}O$ k_{22}

$LMOO + R_2NO + H^+ \rightarrow LMOOH + R_2N^+{=}O$ k_{12}

$LMOO + R_2NO + H^+ = LMOOH + R_2N^+{=}O$ K_{12}

Used known k_{12} for $Cr_{aq}OO^{2+}$ + TEMPO-X and K_{12} from ΔE° = (1.03 V - $R_2N^+{=}O/R_2NO$) to evaluate the product of (k_{11} x k_{22}). Use this estimated $k_{11}k_{22}$ value with the measured k_{12} for $Rh(NH_3)_4(H_2O)OO^{2+}$ + TEMPO-X to evaluate K_{12} and ΔE° for the $Rh(NH_3)_4(H_2O)OO^{2+}$ + TEMPO-X reaction, and E° for $Rh(NH_3)_4(H_2O)OO^{2+}/\text{-}OOH^{2+}$

Table S-1

Nitroxyl	ΔE°Cr	K_{12}Cr	k_{12}Cr	$k_{11}k_{22}$	k_{12}Rh	*calc.* K_{12}Rh	*calc.* ΔE°Rh	E° $RhOO/OOH^{2+}$
TEMPO	0.31 V	1.6×10^5	406	1	104	1.0×10^4	0.236 V	0.95-0.97 V
-OL	0.23 V	7.7×10^3	159	0.33	47	6.7×10^3	0.226 V	1.02-1.03 V
-ONE	0.12 V	1.0×10^2	28	7.84	~5	~3	~.028 V	0.93-0.94 V

CHAPTER III. NUCLEOIPHILIC ASSISTANCE IN OXYGEN-ATOM TRANSFER REACTIONS CATALYZED BY A RHENIUM(V) DITHIOLATE COMPLEX.

Michael J. Vasbinder and James H. Espenson.

Published as *Organometallics* **2004,** *23,* 3355-3358.

Abstract

Oxygen atom transfer from pyridine *N*-oxides (PyO) to triphenylphosphine is catalyzed by MeReO(mtp)PPh_3, **1**, where $mtpH_2$ is 2-(mercaptomethyl)thiophenol, at a rate given by $v = k_c[\mathbf{1}][PyO]^2/[PPh_3]$. When, however, other nucleophiles **N** are added, the rate law becomes $v = k_N[\mathbf{1}][PyO][\mathbf{N}]/[PPh_3]$, and values of k_N correlate with the nucleophilic strength of the added cocatalyst **N**.

Introduction

Oxygen-atom transfer (OAT) reactions are important two electron redox reactions in Nature,[1-4] as well as having a potential use in selective synthetic oxidations.[5-7] They can be generalized as the reaction of an oxygen-atom donor, D, with an oxygen atom acceptor, A.

$$D\text{-}O + A \rightarrow D + A\text{-}O \qquad (1)$$

A specific kind of OAT reaction is the transfer of oxygen atom from an amine-*N*-oxide to a phosphane. Despite the highly exothermic nature of the reaction, and an expected negative free energy of reaction near -260 kJ mol^{-1},[8] these reactions are not seen in the absence of a catalyst. The reaction of pyridine-*N*-oxides with triphenyl phosphine, assuming little entropy change, is just such a kinetically limited exergonic reaction.

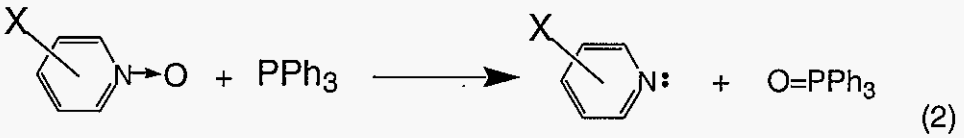

(2)

Triphenylphosphine is a good oxygen-atom acceptor, [9,10] shown by the large P=O bond dissociation energy 557 kJ mol^{-1} for $OPPh_3$.

Kinetics have shown a second-order dependence on pyridine-*N*-oxide O-atom donor in eq 2.[11] It has been suggested that this is due to a nucleophilic attack by a second substrate molecule, after the first O-donor substrate pyridine-*N*-oxide is coordinated. This second order term is always seen in the kinetics regardless of which pyridine-*N*-oxide substrates were used.

Recently, Que and co-workers have reported that the reaction of $Fe^{II}(TPA)(OTf)_2$ where TPA is the tris(pyridyl-2-methyl)amine ligand, with *tert*-butyl hydroperoxide is promoted by nucleophiles.[12] These exogenous nucleophiles were necessary to cleave the $(TPA)Fe^{III}$-OOR intermediate to generate $(TPA)Fe^{IV}$=O species, a model for the active sites of non-heme mononuclear iron enzymes.

The purpose of this study is to quantify this hypothesized nucleophilic assistance. By varying the nucleophilicity of the incoming ligand, it can be seen whether or not this ligand is acting as a nucleophile. It would become convenient to do this via substituent effects. If what is being observed is nucleophilic assistance, then substituents with electron-donating character should enhance the rate of the reaction. Conversely, electron-withdrawing substituents should decrease the reaction rate, by decreasing electron density available for the nucleophile to donate to the reaction center. By studying Hammett linear free energy correlations, this nucleophilic assistance can be quantified.

This mechanistic work follows much work done by researchers in this group. Here the general mechanism of catalysts such as the MeRe(O) mtp-monomer-PPh_3, the catalyst in these particular reactions, has been worked out in detail.

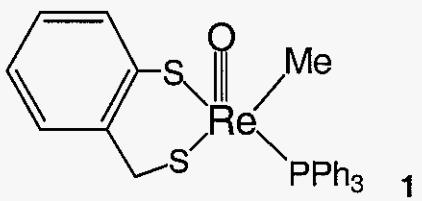

1

This, and the cited previous work allows for the following scheme to be proposed.

Scheme 1.

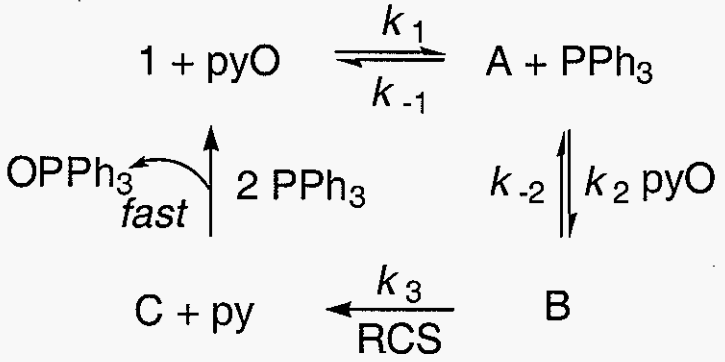

Initially, the PPh_3 ligand is replaced by the incoming oxygen-donating substrate, labeled pyO. This Re^V, 5-coordinate species is then attacked by a nucleophile at the vacant coordination site *trans* to the apical oxo-group. If no exogenous nucleophile is present, this attack can made by a second equivalent of the pyO oxygen-donor substrate. Once this nucleophilic attack, which transfers electron-density into the transition state, happens, the cleavage of the ReO-pyX bond follows. It is this nucleophilic attack which is studied herein.

Experimental

Materials All substituted pyridines, triethylamine, *n*-butyl-imidazole and tetrabutylammonium bromide, as well as the substituted pyridine-*N*-oxides were purchased form Aldrich, and in most cases used without further purification. Spectrophotometric grade DMSO, pyridine and inhibitor-free THF, were purchased from Fisher Scientific and used without further purification. The rhenium catalyst **1** was prepared from the dimeric form, **2,** by stirring the dimer in a benzene solution of PPh_3, following a previously published procedure[13, 14]. Catalyst concentrations were checked spectrophotometrically using known molar absorptivities $\varepsilon_{330\ nm} = 2.6 \times 10^3$ L mol^{-1} cm^{-1} and $\varepsilon_{606\ nm} = 1.9 \times 10^2$ L mol^{-1} cm^{-1}.

Kinetics Reactions were followed spectrophotometrically at convenient wavelengths in the UV absorbance of the substituted pyridine-*N*-oxides, usually between 330-400 nm, using a Shimadzu UV-2101 PC spectrophotometer, or Shimadzu UV-2501 PC spectrophotometer thermostated to 25.0 ± 0.2 °C. All reactions, except those where initial rates were measured, were followed to at least two half-lives. The absorbance-time data were then fit to the following equation:

$$Abs_t = Abs_\infty + (Abs_0 - Abs_\infty) \exp(-k_\psi t) \qquad (3)$$

The values of k_N were then extracted by the following mathematical relationship, assuming the contribution from $k_C[pyO]^2$ is negligible.

$$k_\psi = k_N[Re]_T[nuc][PPh_3]^{-1} \qquad (4)$$

When using 4-piccoline-*N*-oxide as the oxygen-donor substrate, the second-order component could not always be eliminated from the rate law. The resulting kinetic curves were fit to the following equation for mixed first and second-order kinetics.

$$Abs_t = Abs_\infty + \frac{(Abs_0 - Abs_\infty)\, k_{\psi_N} \exp(-k_{\psi_N} t)}{k_{\psi_N} + k_{\psi_C}[pyO]_0\{1 - \exp(-k_{\psi_N} t)\}} \qquad (5)$$

These reactions were followed to completion. Comparisons of fits of mixed order data to eq 3 and 5 are given in the **Supplemental** section (Figure S-1). Values of k_N were obtained by fitting $k_{\psi N}$ vs. nucleophile concentration to the following equation (Figure S-2-6):

$$k_{\psi N}([PPh_3][\mathbf{1}]^{-1}) = k_N[nuc] \qquad (6)$$

Initial rates were determined by converting from absorbance to concentration using the following molar absorptivities for 4-picoline-*N*-oxide $\varepsilon_{330\ nm}$ = 960 L $mol^{-1}cm^{-1}$, 4-nitro-2-methylpyridine-*N*-oxide, $\varepsilon_{390\ nm}$ = 1300 L mol^{-1} cm^{-1} and $\varepsilon_{395\ nm}$ = 670 L mol^{-1} cm^{-1}, and fitting the first 4-5 % of these concentration-time data to a line. In faster reactions, with more scatter in the absorbance data due to the photomultiplier tube[15] or mixing, the full concentration-time profile was fit to a fifth-order polynomial, the derivative of which can be taken, with the second root giving the initial rate [16-17].Values of k_N were obtained using the following relationship, again assuming the contribution from k_N predominates:

$$v_i = k_N[Re]_T[Nuc][pyO][[PPh_3]^{-1} \qquad (7)$$

These values of k_N using either of the two initial rates fitting methods are expected to be reproducible only to ± 15-20%.

Results and Discussion

It has been shown that the rate law for the catalyzed conversion of pyridine-*N*-oxides (pyO) to pyridines is as follows:[11]

$$-d[pyO]/dt = (k_C[pyO] + k_N[Nuc]) [pyO][cat] [PPh_3]^{-1} \qquad (8)$$

This rate law is in complete agreement with what is presented in Scheme 1.

The unusual feature in this rate law is the second-order dependence in pyO concentration to the rate. It was this second-order component that led to the hypothesis of nucleophilic assistance in the reaction mechanism.

Using an excess of an exogenous nucleophile, the reaction can be driven down the k_N path, which is first-order in both nucleophile and substrate. Assuming that the concentrations of the catalyst and nucleophile do not change throughout the course of the reaction, the rate law under *pseudo*-order conditions should be as follows:

$$-d[pyO]/dt = k_{\psi}\,[pyO] \qquad (9)$$

Without an exogenous nucleophile, a *pseudo*-second-order dependence on oxygen-atom donor concentration, 4-picoline oxide in this case, is observed. In the presence of excess Br^-, a *pseudo*-first-order dependence is shown with respect to the concentration of substrate. This based on the slope of the log-log plot of initial rate vs. 4-picoline-*N*-oxide concentration is shown, the slope = 1.0. Bromide was not chosen as a nucleophile in later studies, as it is implicated in catalyst decomposition,[18] which prevents analysis over the full course of the reaction. Also, its nucleophilicity cannot be varied by substitution.

Hammett Correlations

The nucleophilicity of the incoming ligand was varied by adding electron withdrawing and donating substituents to pyridine, then measuring the rate constant as a function of the Hammett substituents parameter, σ. Although nucleophilicity parameters already exist for LFER studies, such as the ones derived from the Edwards[19] and Swain-Scott[20] equations, few nucleophile studies using inorganic systems have been conducted, and there is little correlation between the relative nucleophilicities of metal complexes and organic substrates, such as CH_3I. There are also few correlations between relative nucleophilicities of ligands attacking high-valent metal-oxo species, such as **1**, in comparison to softer, low-valent metal

complexes such as those of Pt^{II}.[21] This necessitated the use of Hammett parameters in order to study relative nucleophilicity.

By varying the substituents on the pyridine, the nucleophilicity of the incoming ligand can be varied. This variation followed the linear fit to the Hammett equation. The slope of this line yielded the Hammett reaction constant for nucleophilic assistance, ρ_N, which was found to be equal to -1.0, where the substrate was 4-nitro-2-methylpyridine-*N*-oxide. ρ_N was found to be –2.7 with 4-picoline-*N*-oxide as the substrate. The significance of this Hammett reaction constant is that the transition state must be more positive than the reaction center, and, consequently, increasing the electron density on the Re-atom increases the rate of the reaction. Previous work has shown a large, negative value for the Hammett reaction constant for the reactions, ρ_C = -3.84.[11] The magnitude is caused by the composite nature of the ρ_C term, due to pyO being involved as a ligand in two binding equilibria and a nucleophile in the rate-determining step. ρ_N represents the Hammett reaction constant for nucleophilic attack, the k_3 step in the proposed mechanism. As such, it is expected to be smaller than the composite term ρ_C of which it is a part.

The Hammett data supports the view of a transition state in which electron density must flow out of the metal complex, supporting the transition state shown in eq 10. As varying the nucleophilicity of the incoming ligand has a direct effect on the rate of the reaction, this nucleophilic assistance step must occur before the rate-controlling cleavage of the ReO-pyX bond.

This can be rationalized in the terms of an oxygen-atom transfer from the substituted pyridine-*N*-oxide to the rhenium complex. An increase in electron density on the rhenium makes it easier for this atom to undergo oxidation, where the more electron-poor rhenium atom, with a less nucleophilic ligand bound, would oxidize more slowly. Chemical intuition and electronegativity tables clearly show that the

new Re=O bond must be polarized towards the oxygen. Also, formal assignment of oxidation states would call for a loss in electron density from Re^{V} to Re^{VII}, agreeing with the Hammett data that electron-density is streaming out of the system. Evidence of the dioxo-Re^{VII} intermediate comes from low-temperature ^{1}H-NMR, where resonances are seen that correspond to this intermediate.[11]

As this reaction has not been observed to occur in the absence of a nucleophilic assistant, in either the form of an exogenous nucleophile, or as the substrate pyridine-*N*-oxide itself, it is clear that the electron density on the rhenium is not sufficient to cause the Re-O-py-X bond cleavage. The Re-center must have an increase in electron density before it can be oxidized to Re^{VII}.

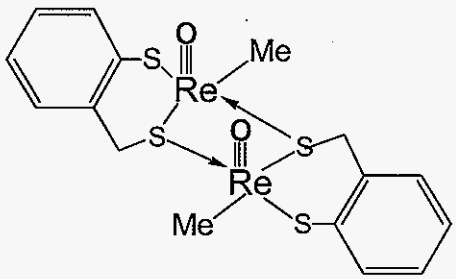

2

A dimeric form of this catalyst, **2,** has recently been shown by our group to have dramatically increased activity, as compared to the monomeric phosphine species **1**. It is more than 90 times faster than **1** in OAT reactions from sulfoxides to PPh_3.[22] This can be rationalized in terms of nucleophilic assistance. The bridging sulfido species acts as an *intra*-molecular nucleophile, eliminating the necessity of inter-molecular coordination of a separate nucleophile. As this inter-molecular nucleophilic attack on the Re-center happens before the hypothesized rate-controlling dissociation of the N-O bond, its elimination should cause an increase in the rate of the reaction. In general, species ligating through sulfur atoms have been shown to be good ligands in our system, as well as being nucleophiles in general. It

provides enough electron density to form the dithiolato-$Re^{VII}(O)_2$ intermediate to be formed.

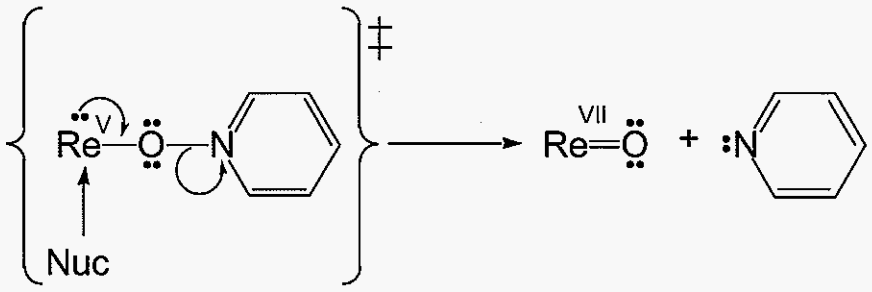

(10)

In the case where 4-piccoline-*N*-oxide was studied as oxygen atom donor and an electron withdrawing pyridine, 4-CN, is used the data point falls well off the line fit by the other data. From the fit to the five electron-donating points, the extrapolated value of k_N for 4-CN would be ~1.4 L mol^{-1} s^{-1}, >10^4 times slower than the self-assisted, k_c reaction. This precludes any accurate measurement of the exogenous nucleophile path, as experimental conditions allowing measurements under the extreme excess of pyridine are unavailable.

Extreme Nucleophile Concentrations

With 4-picoline-*N*-oxide as the substrate, studies were done using an extreme excess of the exogenous nucleophile pyridine, up to 4.9 mol L^{-1}. Under these conditions, the reaction should be forced down the nucleophilic assistance, k_N governed, path. That is, no significant contribution to the rate of X-pyridine-*N*-oxide disappearance is made by the self-assisted, k_C governed path. This could be realized with 4-nitro-2-methylpyridine-*N*-oxide as the substrate, and was evident in the excellent fit to *pseudo*-first-order kinetics (eq 3). However, in the cases where 4-picoline-*N*-oxide is the substrate, only under dramatic excess of nucleophile was a fit to *pseudo*-first-order kinetics observed. This necessitated the fit of time-course kinetic data to eq 5.

In experiments with this dramatic excess of nucleophile, a rapid decrease in Abs. is observed at 330 nm, typical of reactions carried out under smaller excesses of nucleophile, as shown in Fig. 4. Unlike reactions carried out with small py concentrations, a sudden increase in absorbance was observed upon what appeared initially to be the end of the reaction.

We believe the rapid step is the disappearance of pyO to py. However, we were unable to determine to what extent the pyO to py reaction occurred, due to the uncertainty in the endpoint in the reaction.

This implies high pyridine concentrations can change the observed Abs_∞. The increase in Abs_∞ that could be seen in the timecourse at 330 nm is consistent with the formation of a Re-py species, which has a molar absorptivity at that wavelength greater than the Re-PPh_3 complex.[23] Control experiments, done by addition of excess pyridine *after* the reaction had completed, showed no increase in absorbance, indicating that the reaction yielding the rapid absorbance increase was between pyridine and an intermediate species, not the products of the reaction. Also, pyridine will not undergo apparent ligand exchange with Re-PPh_3. In fact the microscopic reverse, Re-py being displaced by PPh_3, goes to completion on the stopped-flow timescale.[23] This ligand displacement most likely occurs in the last step of the mechanism, where phosphine oxide is displaced by another incoming ligand. In the absence of these extremely high pyridine concentrations, another PPh_3 molecule enters displacing the product of the OAT reaction, $OPPh_3$, and regenerating starting catalyst **1**.

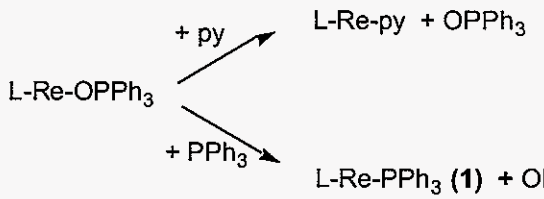

The ligand exchange between $OPPh_3$ and PPh_3/py has not been directly observed for these Re-complexes, but we expect it to be facile, due to the relative basicities of the species involved, and due to the fact that no Re-$OPPh_3$ species has ever been isolated, whereas dozens of Re-PPh_3 and Re-py species have been prepared by the action of the ligands on dimeric rhenium complexes such as **2**.

Nucleophiles Other Than Substituted Pyridines

Various other nucleophiles including THF, DMSO, *N-n*-butyl-imidazole, and triethylamine, were used throughout the course of the study, and results are summarized in Table 1.

THF was shown to have no effect on the order of the reaction with respect to the oxygen-donating pyridine-*N*-oxide substrate. In other words, no evidence for the exogenous nucleophile path was seen, as the reaction remained second-order in pyridine-*N*-oxide. This was interpreted to the low nucleophilicity of THF; the interaction of THF and the transition state does not afford enough electron density to form the new Re=O bond in the high-energy rhenium(VII) intermediate. High THF/pyO ratios did not affect the second-order term in pyO.

The use of the imidazole derivative was significant, because of its availability as a biological ligand in the form of the amino acid histidine. As OAT processes occur in Nature, the interest in biologically analogous ligands becomes apparent. Recently, imidazole and other *N*-heterocycles have been studied [24] in the monomerization of dimer species **2**. It was found that imidazole favors formation of monomer, with a large equilibrium constant for monomerization, K_{eq}, $>10^5$. This implies that imidazole binds tightly to the Re-center, stimulating interest in determining weather or not imidazole would serve as a nucleophile. The lack of solubility of imidazole and histidine in benzene prevented their direct study in this system; *N-n*Bu-imidazole was used because of its greater solubility in benzene. The

k_N for *n*Bu-imidazole was shown to be 2.60 ± 0.13 L mol^{-1} s^{-1}, which makes it a relatively good nucleophile in this system. However, the electron-donating nature of the *n*Bu- group should inductively add more electron density to the ligating N-atom, probably increasing the nucleophilicity of this ligand with respect to ordinary imidazole.

Dimethyl sulfoxide is an interesting choice of nucleophile, in that it ligates through an oxygen atom instead of nitrogen. Dithiolato-(Me)Re^{V}O complexes of the type studied are well known for their oxophilicity, the differing nucleophilicities of pyridine-*N*-oxides as compared to pyridines are one example. We were interested in the acceleration caused by O-coordination as opposed to N-coordination. In other studies done by our group, DMSO has been used as an oxygen-atom donor in OAT reactions.[25] It was hoped that this background reaction would not obscure the interpretation of the nucleophilicity of DMSO. Unfortunately, under the conditions necessary to guarantee the nucleophilic assistance path dominates, which calls for excess DMSO, the rate of this DMSO-PPh_3 OAT reaction became competitive with the ordinarily faster pyridine-*N*-oxide reaction, especially when using the slowly reacting 4-nitro-2-methylpyridine-*N*-oxide as the oxygen-donating substrate. Still, based upon initial rate studies, the k_N is estimated to be 1.20 ± 0.18 L mol^{-1} s^{-1}, roughly as nucleophilic as an alkyl substituted pyridine.

Triethylamine, the strongest base used, was shown to proceed more slowly than any of the other nucleophile promoted reactions. Based upon initial rate studies, the k_N for triethylamine is estimated to be 0.08 L mol^{-1} s^{-1}. Less than 70% of the pyridine-*N*-oxide will travel down the triethylamine-assisted path under the conditions employed, necessitating the use of initial rates.

Triethylamine has steric considerations when binding to a metal center. It has a larger cone angle[26] than triphenylphosphine[27], which would hinder nucleophilic

attack on the catalyst-Opy intermediate. There was no evidence of adduct formation between triethylamine and the catalyst. Studies of this amine with the dimer form, **2**, of the catalyst showed no monomerization, evident from the lack of a distinct band near 600-650 nm attributed to the monomer form of the catalyst.

Conclusions

The effect of added nucleophiles on the $MeReO(mtp)PPh_3$ catalyzed oxygen-atom transfer reaction from pyridine-*N*-oxides to triphenylphosphine is summarized in Scheme 2. The rate law for the reaction in the absence of added nucleophile **N** was $v = k_c[\mathbf{1}][PyO]^2/[PPh_3]$. When other nucleophiles are added, the rate law become $v = k_N[\mathbf{1}][PyO][\mathbf{N}]/[PPh_3]$. The magnitude of k_N is proportional to the Hammett substituent constant σ. The Hammett reaction constants ρ_N were found to be -1.0(1) for 4-nitro-2-methylpyridine-*N*-oxide and -2.6(4) for 4-methylpyridine-*N*-oxide as oxygen-donor substrates. The data for the series of nucleophiles are summarized in Table 1. The values of ρ_N can be compared with ρ_C = -3.84 for XC_5H_4NO.[11] Note that ρ_N can be factored into two components, one for the XC_5H_4NO substrate and the other for the XC_5H_4NO nucleophile: $\rho_C = \rho_{C,sub.} + \rho_{C,nucl.}$ One can further assume that the nucleophilic component is smaller (less negative) than $\rho_{N,Py}$ = -2.6 because the ring substituent X is one atom further removed from the rhenium atom reaction center. An estimate of is $\rho_{C,sub.}$as -3.8 - (<-2.6), implying that $\rho_{C,sub.}$ is more negative than -1.2. These are not unreasonable reaction constants; one might not be far amiss in suggesting that ρ_C comprises two negative contributions of roughly similar magnitudes.

Interestingly, the best nucleophiles for the MeReO(mtp)PPh_3 catalyst seem to be the pyridine-*N*-oxide oxygen-donor substrates themselves. A relatively large amount of exogenous nucleophile must be added to significantly drive the reaction down the k_N pathway. Similar results were seen by Que et al in the (TPA)Fe^{III}-OOR/(TPA)Fe^{IV}=O system, where the pyridine-*N*-oxide nucleophile drove the reaction an order of magnitude faster than 4-dimetylaminopyridine.[12]

Scheme 2.

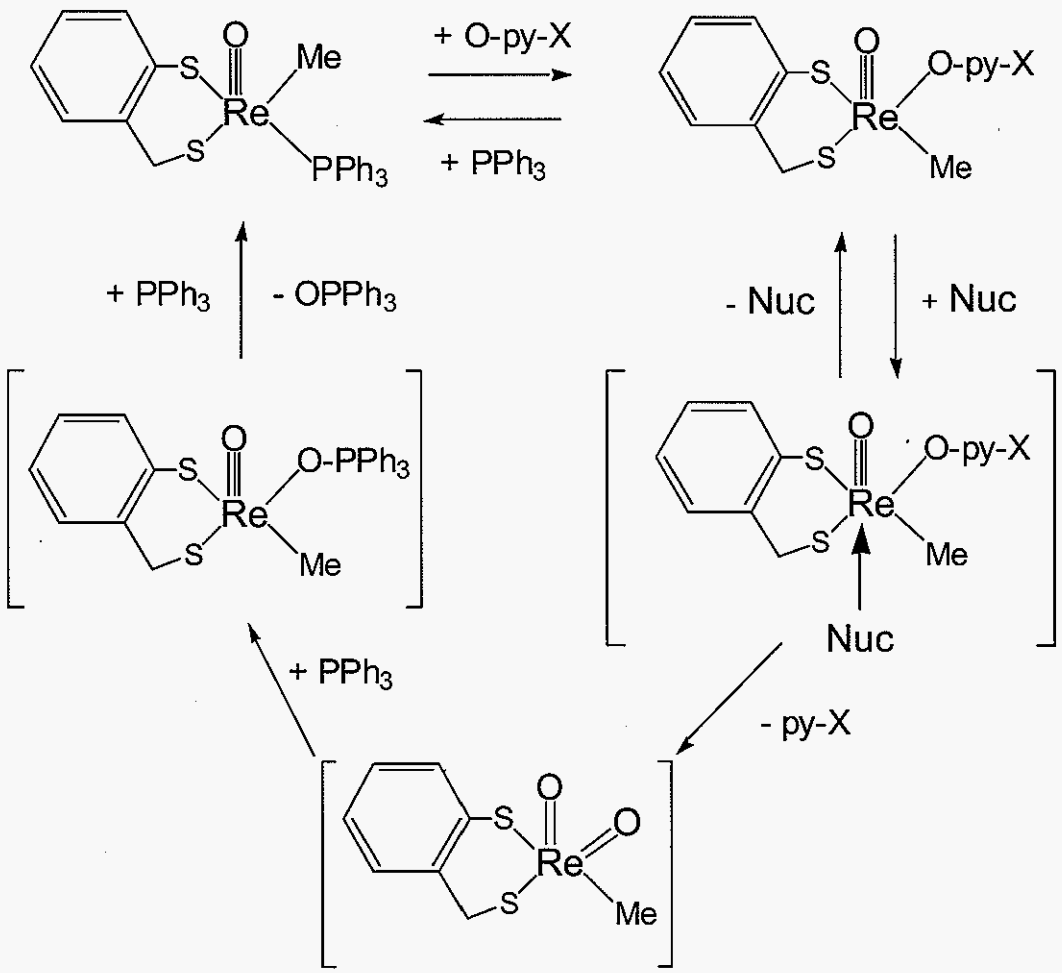

Table 1. Rate Constants for the Nucleophile-Assisted Reactions between Pyridine *N*-Oxides and Triphenyl Phosphine

	k_N/L mol^{-1} s^{-1}		
nucleophile	4-NO_2-2-MeC_5H_3NO	4-MeC_5H_4NO	σ [a]
pyridines			
4-$Me_2NC_5H_4N$	4.25(21)		-0.83
4-$MeOC_5H_4N$	1.90(10)	421(6)	-0.27
4-*t*-BuC_5H_4N	1.33(7)	375(20)	-0.2
4-MeC_5H_4N	1.05(5)	194(10)	-0.17
3-MeC_5H_4N	1.01(5)		-0.07
4-PhC_5H_4N	0.92(5)	107(9)	-0.01
C_5H_5N	0.73(4)	77(3)	0
3-ClC_5H_4N	0.47(9)		0.15
3-NCC_5H_4N	0.18(4)		0.55
4-NCC_5H_4N	0.15(2)	119(7)	0.66
pyridine *N*-oxides			
4-NO_2-2-MeC_5H_3NO	1		
4-$NO_2C_5H_4NO$	(1.78) [b]		
4-MeC_5H_4NO		1.50(1) × 10^4	
others			
$[NBu_4]Br$		4.0(6) × 10^3	
n-Bu-imidazole	2.60(13)		
Me_2SO	1.2(2)		
NEt_3	0.08(2)		
THF	no effect		

[a] Taken from Ref. 28.

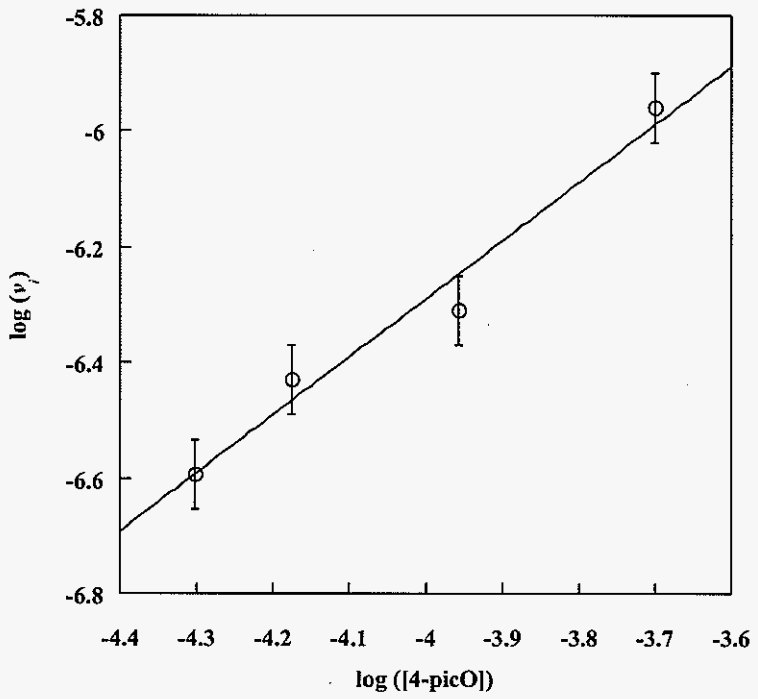

Figure 1. log-log plot of the initial rate of oxygen-donor disappearance at various starting concentrations of oxygen-donor. Order = Slope = 1.00 ± 0.12, R = .98. Conditions: [**1**] = 8-9 x 10^{-6} mol L^{-1}; [PPh_3] = 2.0 x 10^{-2} mol L^{-1} ; [NBu_4Br] 1.0 x 10^{-3} mol L^{-1} .

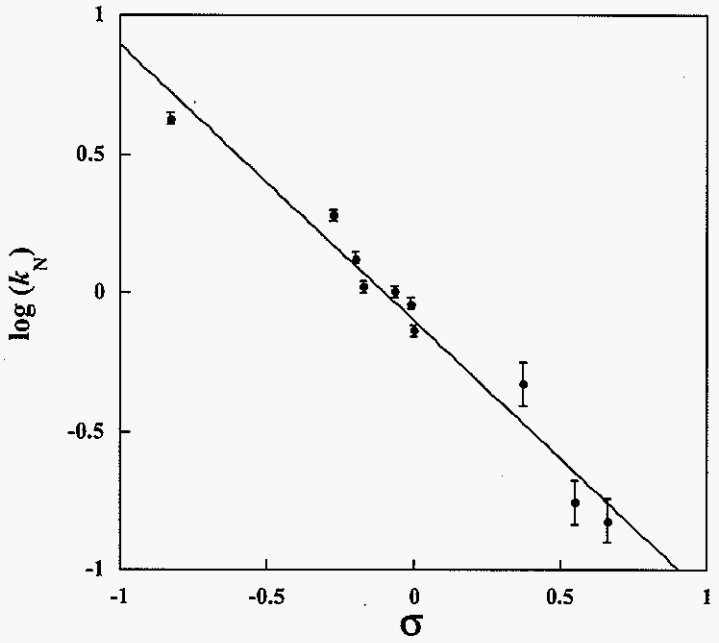

Figure 2. Hammett LFER for various 4-X-pyridine nucleophiles, for the overall reaction of 4-NO_2-2-Me-pyridine-*N*-oxide and PPh_3, in benzene at 25 ° C. Slope = $\rho = -1.0 \pm 0.07$.

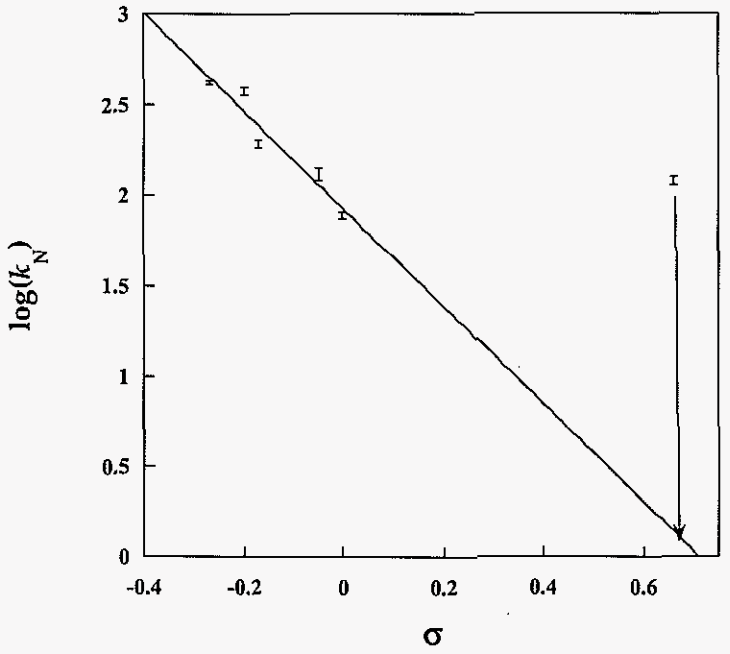

Figure 3. Hammett LFER for various 4-X-pyridine nucleophiles for the overall reaction of 4-piccoline-*N*-oxide and PPh_3, in benzene at 25 °C. Slope = $\rho = -2.7 \pm 0.4$. The arrow is drawn to emphasize the predicted position of the 4-CN substituted pyridine. Its value was not included with the other five points in the linear fit.

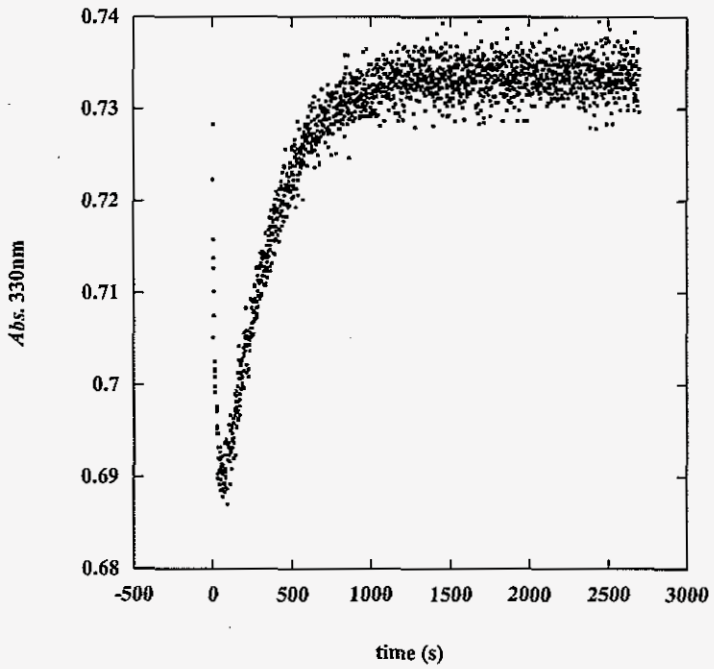

Figure. 4 Reaction of 4-piccoline-N-oxide as substrate with an extreme exogenous pyridine nucleophile excess. Conditions: [**1**] = 2 x 10^{-5} mol L^{-1}; [PPh_3] = 2.5 x 10^{-2} mol L^{-1}; [pyridine] 4.9 mol L^{-1} ; [picO] = 2 x 10^{-4} mol L^{-1}.

References

(1) Hille, R. *Chem. Rev.* **1996**, *96*, 2757-2816.

(2) Holm, R. H. *Chem. Rev.* **1987**, *87*, 1401-49.

(3) Holm, R. H.; Berg, J. M. *Acc. Chem. Res.* **1986**, *19*, 363-70.

(4) Li, H.; Palanca, P.; Sanz, V.; Lahoz, L. In *Inorg. Chim. Acta* **1999**, *285*, 25-30.

(5) Owens, G. S.; Arias, J.; Abu-Omar, M. M. *Catal. Today* **2000**, *55*, 317-363.

(6) Romão, C. C.; Kühn, F. E.; Herrmann, W. A. *Chem. Rev.* **1997**, *97*, 3197-3246.

(7) Wang, Y.; Espenson, J. H. *Org. Lett.* **2000**, *2*, 3525-3526.

(8) Ribeiro da Silva, M. D. M. C.; Agostinha, M.; Matos, R.; Vaz, M. C.; Santos, L. M. N. B. F.; Pilcher, G.; Acree, W. E., Jr.; Powell, J. R. *J. Chem. Thermodyn.* **1998**, *30*, 869-878.

(9) Holm, R. H.; Donahue, J. P. *Polyhedron* **1993**, *12*, 571-589.

(10) Moyer, B. A.; Sipe, B. K.; Meyer, T. J. *Inorg. Chem.* **1981**, *20,* 1475-1480.

(11) Wang, Y.; Espenson, J. H. *Inorg. Chem.* **2002**, *41*, 2266-2274.

(12) Kaizer, J.; Costas, M.; Que, L., Jr. *Angew. Chem., Int. Ed.* **2003**, *42*, 3671-3673.

(13) Jacob, J.; Guzei, I. A.; Espenson, J. H. *Inorg. Chem.* **1999**, *38*, 1040-1041.

(14) Lente, G.; Guzei, I. A.; Espenson, J. H. *Inorg. Chem.* **2000**, *39*, 1311-1319.

(15) Skoog, D. A.; Holler, F. J.; Nieman, T. A. *Principles of Instrumental Analysis*; 5th ed.; Saunders: Philadelphia, **1998**. p 309

(16) Espenson, J. H. *Chemical Kinetics and Reaction Mechanisms*; 2 ed.; McGraw Hill, Inc.: New York, pp 19, 24, **1995**.

(17) Hall, K. J.; Quickenden, T. I.; Watts, D. W. *J. Chem. Educ.* **1976**, *53*, 493.

(18) Saha, B.; Espenson, J. H. unpublished resutls.

(19) Edwards, J. O. *J. Am. Chem. Soc.* **1956**, *78*, 1819-1820.

(20) Swain, C. G; Scott, C. B. *J. Am. Chem. Soc.* **1953**, *75*, 141-147.

(21) Pearson, R. G; Sobel, H.; Longstad, J. *J. Am. Chem. Soc.* **1968**, *90*, 319-326.

(22) Koshino, N.; Espenson, J. H. *Inorg. Chem.* **2003**, *42*, 5735-5742.

(23) Lahti, D. W.; Espenson, J. H. *J. Am. Chem. Soc.* **2001**, *123*, 6014-6024.

(24) Espenson, J. H.; Nabavizadeh, S. M. *Eur. J. Inorg. Chem.* **2003**, 1911-1916.

(25) Lente, G.; Espenson, J. H. *Inorg. Chem.* **2000**, *39*, 4809-4814.

(26) Seligson, A. L.; Trogler, W. C. *J. Am. Chem. Soc.* **1991**, *113*, 2520-2527.

(27) Tollman, C. A. *Chem. Rev.* **1977**, *77*, 313-348.

(28) Hansch, C.; Leo, A.; Taft, R. W. *Chem. Rev.* **1991**, *91*, 165-195.

Supplemental

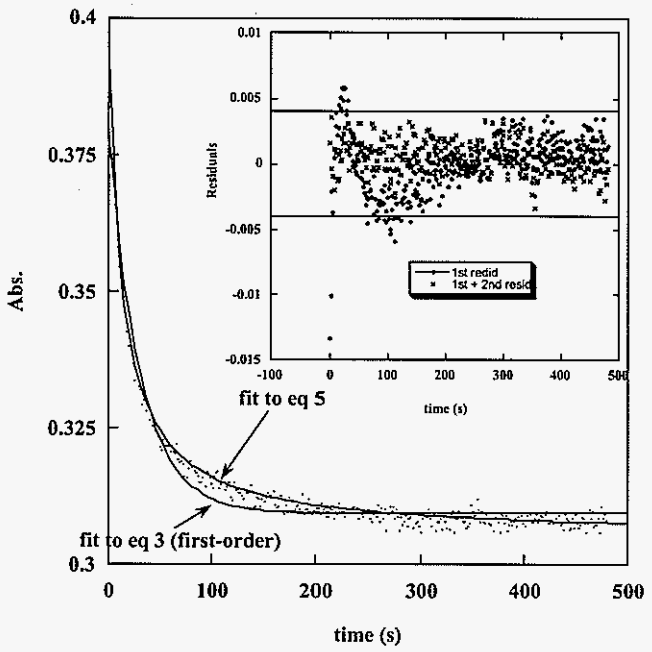

Figure S-1. Abs-time trace showing fits to pure first-order and mixed first and second order kinetics. Conditions: [**1**] = 1.7 x 10^{-5} mol L^{-1}; [PPh_3] = 1.95 x 10^{-2} mol L^{-1} ; [pyridine] = 0.124 mol L^{-1} , [4-piccoline-*N*-oxide] = 2.1 x 10^{-4} mol L^{-1}. **Inset** Shows the residuals vs. time of the two respective fits, mixed-order with × and first-order with ◊. The horizontal lines represent typical limits of noise for the instrument, roughly ± .004 Abs units.

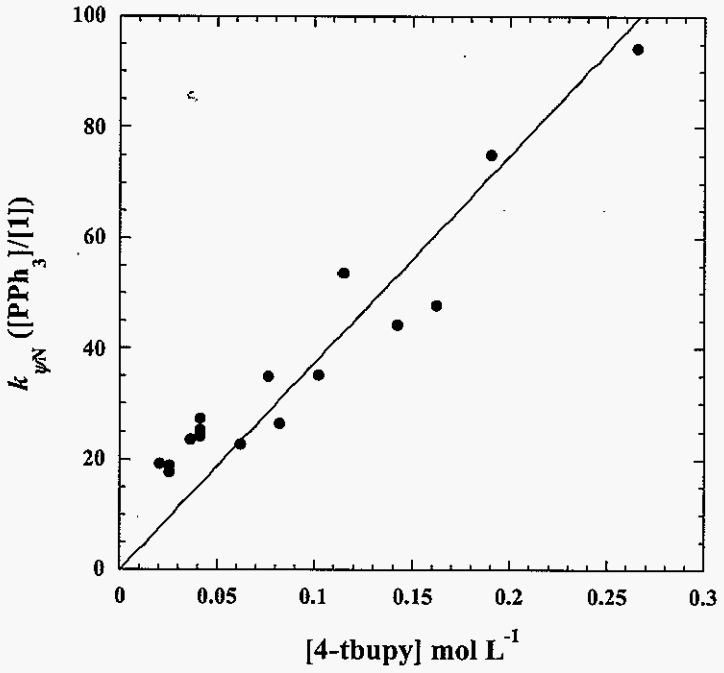

Figure S-2. Fit to $k_{\psi N}$ ([PPh_3][**1**]$^{-1}$) = k_N[nuc]. Slope = k_N = 375 ± 20. Conditions: [**1**] = 1.7 x 10^{-5} mol L^{-1}; [PPh_3] = 1.9-2.0 x 10^{-2} mol L^{-1}; [4-piccoline-*N*-oxide] = 2.1 x 10^{-4} mol L^{-1}.

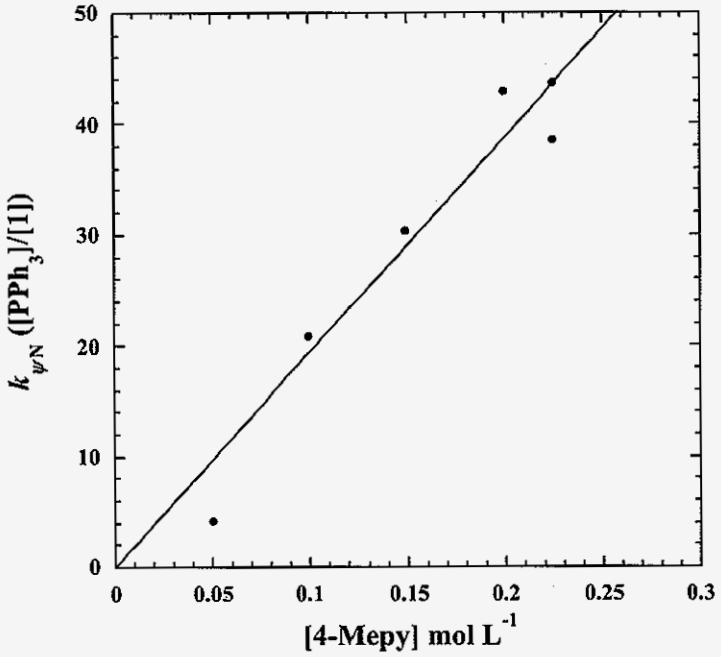

Figure S-3. Fit to $k_{\psi N}$ ([PPh_3][**1**]$^{-1}$) = k_N[nuc]. Slope = k_N = 194 ± 10. Conditions: [**1**] = 1.7 x 10^{-5} mol L^{-1}; [PPh_3] = 1.9-2.0 x 10^{-2} mol L^{-1} ; [4-piccoline-*N*-oxide] = 2.1 x 10^{-4} mol L^{-1}.

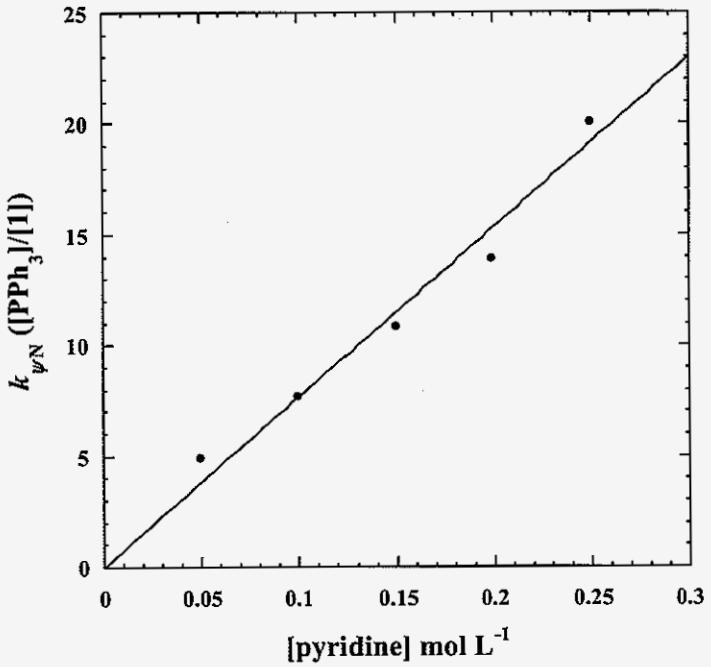

Figure S-4. Fit to $k_{\psi N}$ ([PPh_3][**1**]$^{-1}$) = k_N[nuc]. Slope = k_N = 77 ± 3. Conditions: [**1**] = 1.7 x 10^{-5} mol L^{-1}; [PPh_3] = 1.9-2.0 x 10^{-2} mol L^{-1} ; [4-piccoline-*N*-oxide] = 2.1 x 10^{-4} mol L^{-1}.

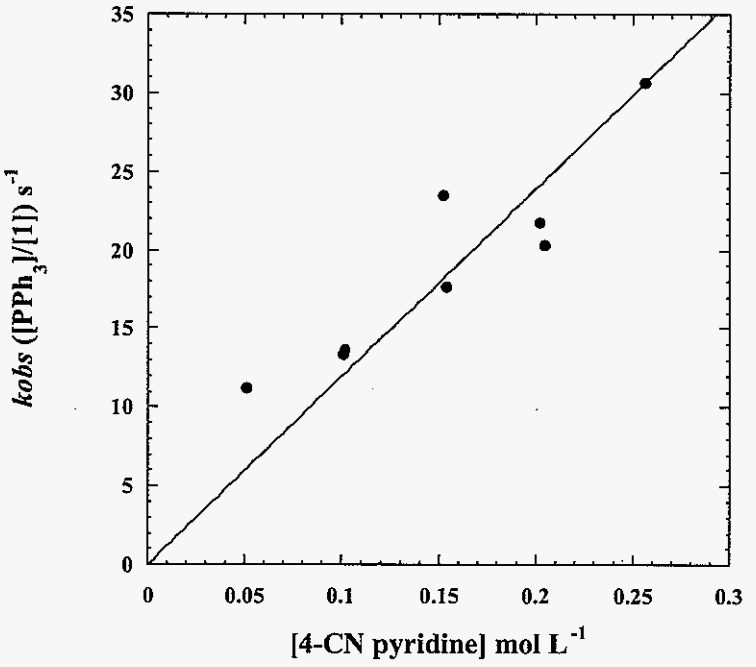

Figure S-5. Fit to $k_{\psi N}$ ([PPh_3][**1**] $^{-1}$) = k_N[nuc]. Slope = k_N = 119 ± 7. Conditions: [**1**] = 1.7 – 2.5 x 10^{-5} mol L^{-1}; [PPh_3] = 1.9-2.0 x 10^{-2} mol L^{-1} ; [4-piccoline-*N*-oxide] = 2.1 x 10^{-4} mol L^{-1}.

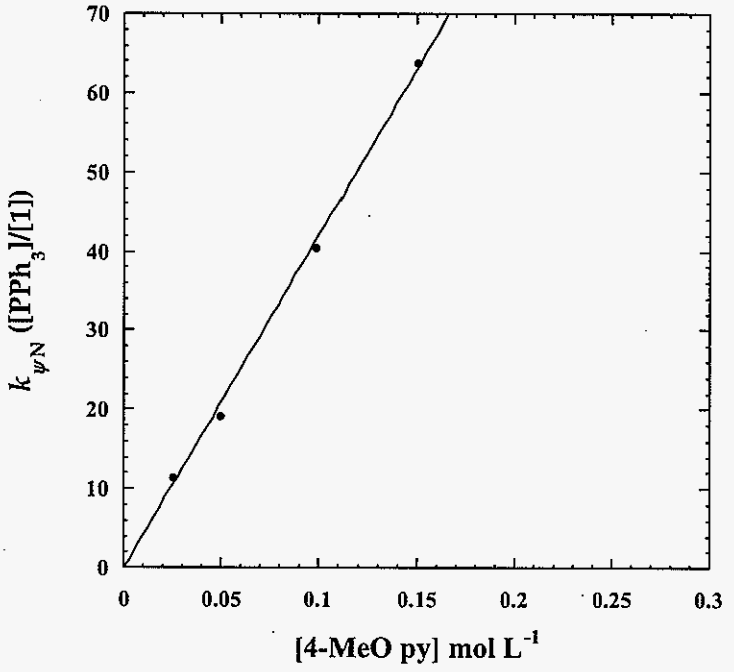

Figure S-6. Fit to $k_{\psi N}$ ([PPh_3][**1**]$^{-1}$) = k_N[nuc]. Slope = k_N = 421 ± 6 Conditions: [**1**] = 1.7 x 10^{-5} mol L^{-1}; [PPh_3] = 1.9-2.0 x 10^{-2} mol L^{-1} ; [4-piccoline-*N*-oxide] = 2.1 x 10^{-4} mol L^{-1}.

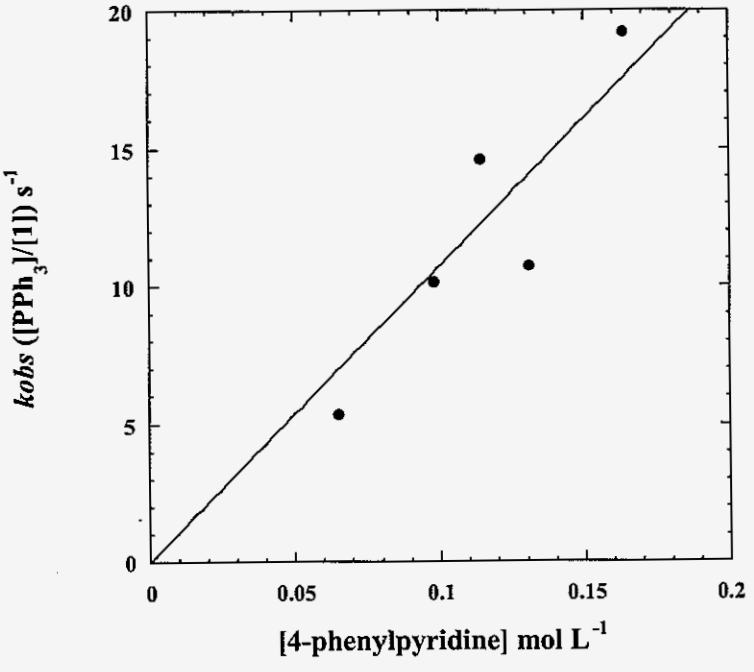

Figure S-7. Fit to $k_{\psi N}([PPh_3][\mathbf{1}]^{-1}) = k_N[nuc]$. Slope = k_N = 107 ± 9. Conditions: [**1**] = 1.7 x 10^{-5} mol L^{-1}; [PPh_3] = 1.5-2.0 x 10^{-2} mol L^{-1} ; [4-piccoline-*N*-oxide] = 2.1 x 10^{-4} mol L^{-1}.

GENERAL CONCLUSIONS

Chapters I and II dealt with the chemistry of superoxo-, hydroperoxo-, and oxo- complexes of chromium, rhodium and cobalt. Chapter III dealt with the mechanism of oxygen-atom transfer catalyzed by an oxo-complex of rhenium.

In Chapter I, it was shown that hydroperoxometal complexes of cobalt and rhodium react with superoxochromium and chromyl ions, generating reduced chromium species while oxidizing the hydroperoxometal ions to their corresponding superoxometal ions. It was shown that the chromyl and superoxochromium ions are the more powerful oxidants. Evidence supports hydrogen atom transfer from the hydroperoxometal ion to the oxidizing superoxochromium or chromyl ion as the reaction mechanism. There is a significant H/D kinetic isotope effect. Comparisons to the rate constants of other known hydrogen atom transfer reactions show the expected correlation with bond dissociation energies.

In Chapter II, it was found that the superoxometal complexes $Cr_{aq}OO^{2+}$ and $Rh(NH_3)_4(H_2O)OO^{2+}$ oxidize stable nitroxyl radicals of the TEMPO series with rate constants that correlate with the redox potentials of both the oxidant and reductant. These reactions fit the Marcus equation for electron transfer near the theoretical value. Acid catalysis is important to the reaction, especially the thermodynamically limited cases involving $Rh(NH_3)_4(H_2O)OO^{2+}$ as the oxidant. The rate constants are notably less than those measured in the reaction between the same nitroxyl radicals and other strong free-radical oxidants, an illustration of the delocalized and stabilized nature of the superoxmetal ions.

Chapter III showed that oxo-rhenium(V) catalysts needed a nucleophile to complete the catalytic oxygen-atom transfer from substituted pyridine-*N*-oxides to triphenylphosphine. The reaction was studied by introducing various pyridine-derived nucleophiles and monitoring their effect on the rate, then fitting the observed rate

constants to the Hammett correlation. It was found that the values of the Hammett reaction constant ρ_N were -1.0(1) for 4-nitro-2-methylpyridine-*N*-oxide and -2.6(4) for 4-methylpyridine-*N*-oxide as substrates. The negative value confirms pyridine is acting as a nucleophile. Nucleophiles other than pyridine derivatives were also tested. In the end, it was found that the most effective nucleophiles were the pyridine-*N*-oxides themselves, meaning that a second equivalent of substrate serves as the most efficient promoter of this oxygen-atom transfer reaction. This relative nucleophilicity of pyridines and pyridine-*N*-oxides is similar to what is observed in other OAT reactions generating high-valent metal-oxo species.

ACKNOWLEDGMENTS

I would like to thank my Major Professors, Drs. Andreja Bakac and James H. Espenson for their ideas, advice, assistance and general mentorship during the course of my studies.

I am grateful to all the past and present members of the Bakac and Espenson groups, who provided a very helpful, friendly, stimulating, and altogether enjoyable working environment over the years. Special thanks go to Dr. Oleg Pestovsky for many helpful discussions and expert training in the preparation of several compounds studied in this dissertation.

Finally, I would like to thank my family and friends, especially my parents and wife Amie Yang for their unwavering support during the course of my education. Without them this work would not have been possible.

This research was supported by the U.S. Department of Energy, Office of Basic Energy Sciences, Division of Chemical Sciences, under contract W-7405-Eng-82 with Iowa State University of Science and Technology. The United States government has assigned the DOE Report number IS-T 2327.